



ELSEVIER

Tectonophysics 252 (1995) 61–101

TECTONOPHYSICS

# Palaeostress reconstructions and geodynamics of the Baikal region, Central Asia, Part I. Palaeozoic and Mesozoic pre-rift evolution

D. Delvaux<sup>a,\*</sup>, R. Moeys<sup>b</sup>, G. Stapel<sup>b</sup>, A. Melnikov<sup>c</sup>, V. Ermikov<sup>d</sup>

<sup>a</sup> Royal Museum for Central Africa, Department of Geology–Mineralogy, B-3080 Tervuren, Belgium

<sup>b</sup> Free University of Amsterdam, De Boelelaan, 1085, 1081 HV Amsterdam, Netherlands

<sup>c</sup> Institute of the Earth's Crust, Lermontov st., 128, 664033 Irkutsk, Russia

<sup>d</sup> United Institute of Geology, Geophysics and Mineralogy, 630090 Novosibirsk, Russia

Received 21 April 1994; accepted 16 January 1995

## Abstract

This paper presents the first palaeostress results obtained for the basement of the Baikal rift system, in southern Siberia (Russia). Large-scale structural analysis and palaeostress reconstructions show that the Palaeozoic–Mesozoic kinematic history, precursor of the Baikal Cenozoic rifting, is characterized by the succession of six regional palaeostress stages. Stress inversion of fault-slip data and earthquake focal mechanisms is performed using an improved right-dieder method, followed by rotational optimization (D. Delvaux, TENSOR program). The results are interpreted in the light of recent developments in the investigation of regional intraplate stress field, and used as additional constraints for palaeogeodynamic reconstruction of Central Asia.

After the final Palaeozoic closure of the Palaeo-Asian ocean on the southern margin of the Siberian platform, the marginal suture with the Sayan–Baikal Caledonian belt was repeatedly and preferentially reactivated during the subsequent Palaeozoic and Mesozoic history. This suture zone also controlled the opening of the Baikal rift system in the Cenozoic. The progressive closure of the Palaeo-Asian and Mongol–Okhotsk oceans generated successive continental collisions, which were recorded in the Baikal area by brittle–ductile and brittle deformations. The first two palaeostress stages correspond to the successive collage of Precambrian microcontinents and Caledonian terranes along the southern margin of the Siberian platform: (1) Late Cambrian–Early Ordovician N–S compression; and (2) Late Silurian–Early Devonian NW–SE compression. The next two stages are related to the remote effects of the complex evolution of the western Palaeo-Asian ocean, southwest of the Siberian continent: (3) Late Devonian–Early Carboniferous N–S compression, recorded only in the Altai region; and (4) Late Carboniferous–Early Permian E–W compression, recorded both in the Altai and Baikal regions. The last stages are the consequences of the Mongol–Okhotsk oceanic closure: (5) Late Permian–Triassic NW–SE extension with development of Cordilleran-type metamorphic core complexes and volcanism along the active margin of the Mongol–Okhotsk ocean; (6) initial development of Early–Middle Jurassic 10–15-km-wide molassic basins in Trans-Baikal and large foredeeps along the southern margin of the Siberian platform in probable extensional context, but for which no palaeostress data are available; and (7) final closure of the Mongol–Okhotsk ocean in the Cretaceous. This last event resulted from the collision between the Mongol–China and the Siberian plates and is evidenced by the inversion of the Middle

\* Corresponding author.

Mesozoic basins and by Late Jurassic–Early Cretaceous coal-bearing sedimentation in Trans-Baikal. This long tectonic history yielded a highly heterogeneous basement in the Baikal area, precursor of the Cenozoic rifting.

## 1. Introduction

Continental rift zones typically develop along zones of crustal weakness, associated with long-existing discontinuities, as a consequence of their reactivation under an applied stress field. The stress field often evolves during rift history, under a process control both inherent and external to rifting. Therefore, a comprehensive investigation of the geodynamics of rifting requires a triple approach, involving the genesis of pre-rift structural discontinuities, the history of rift-related stress field evolution and its

effects on the existing discontinuities. Examples of modification of the kinematic regime during rift evolution, by inversion or rotation of stress axes are the Rhine Graben–North Sea rift system (Illies, 1972; Ziegler, 1992), the Red Sea–Gulf of Suez system (Joffe and Garfunkel, 1987; Ott d'Estevou et al., 1989), the East-African rift system (eastern branch: Strecker et al., 1990; Bothworth et al., 1992; western branch: Delvaux et al., 1992; Ring et al., 1992), and the Baikal rift system (Logatchev and Zorin, 1987, Logatchev and Zorin, 1992).

The Baikal rift system is situated at the southern

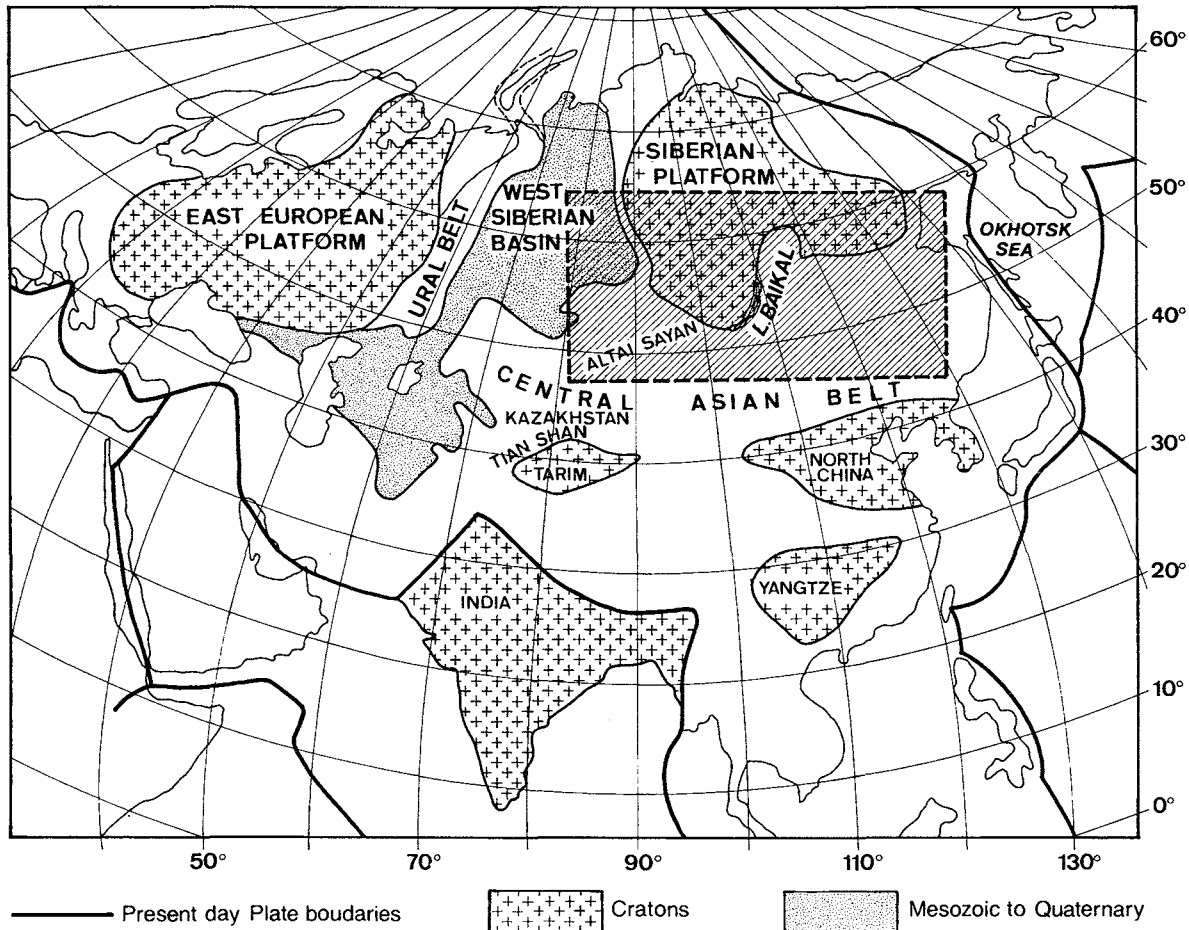


Fig. 1. Location of the Baikal area in Central Asia, with major geodynamic subdivisions and area covered by Fig. 2.

margin of the Siberian platform, along the suture with the Central Asian fold belt (Fig. 1). This marginal zone has been subjected to repeated tectonic movements and major reactivations during its Late Proterozoic and Phanerozoic history. The pre-rift kinematic history of the Baikal rift zone is mainly linked to the evolution of the Central Asian fold belt, related to Palaeo-Asian and Mongol–Okhotsk oceanic evolution. It started by the initial opening of the Palaeo-Asian ocean in the Late Proterozoic, with the development of a passive continental margin along the southern margin of the Siberian Platform, and ended by the final closure of the Mongol–Okhotsk ocean in the Cretaceous. The brittle–ductile conditions of deformation established in the Early Palaeozoic and purely brittle conditions prevailed since the end of the Early Palaeozoic. During this long history, repeated faulting occurred in the Baikal area, mainly related to compressive or transpressive stress fields.

The Cenozoic history in the Baikal area started in the Eocene, contemporaneously with the India–Eurasia collision, and after a long period of tectonic stability and planation in the Late Cretaceous–Paleocene (Molnar and Tapponnier, 1975; Logatchev and Florensov, 1978). The planation surface, characterized by a kaolinite–laterite horizon, defines a clear reference surface which allows to differentiate between pre-rift and rift movements (Logatchev, 1993; Kashik and Mazilov, 1994).

The Baikal rift system evolved in a succession of three tectonic stages, subsequently to an initial stage of tectonic stability with intense chemical weathering, which result in the development of a the Late Cretaceous–Palaeogene peneplain. In Eocene–Early Oligocene time, initial destabilisation along the margin of the Siberian craton caused the development of early depocentres in the southern part of the future rift system. Rifting started in Middle Oligocene by the ‘slow rifting stage’, and evolved recently into the present ‘fast rifting stage’, initiated in Middle–Late Pliocene (Logatchev and Zorin, 1987; Logatchev, 1993). The ongoing tectonic activity is evidenced by the high seismicity. Earthquake focal mechanisms indicate that an extensional regime prevails over most of the Baikal rift zone (Zonenshain and Savostin, 1981; Déverchère et al., 1993).

This work aims at the reconstruction of geody-

namic and palaeostress evolution of the Baikal rift region, in function of the intracontinental setting in Central Asia. It presents the first results of a large-scale investigation of palaeostress and present-stress evolution of the Baikal rift area, for the whole pre-rift and rifting periods, using the method of stress tensor reconstruction from brittle microstructures and from earthquake focal mechanisms. It is based on field work in 1991, 1992 and 1993 along the whole western coast of Lake Baikal and in the Trans-Baikal area, south of Lake Baikal, jointly with the Royal Museum for Central Africa and the Earth’s Crust Institute of Irkutsk. In 1993, the team was enlarged by participants of the Free University of Amsterdam and the United Institute of Geology, Geophysics and Mineralogy of Novosibirsk.

Due to the strong influence of the pre-rift tectonic inheritance, the Cenozoic tectonic evolution cannot be properly understood without a comprehensive knowledge of the pre-Cenozoic history of Central Asia. Therefore, this work is presented in two different parts. This paper concentrates on the pre-rift evolution, with palaeostress reconstructions for the Palaeozoic and Mesozoic periods and related geodynamic evolution. Another paper (Delvaux et al., submitted) presents the Cenozoic evolution of stress fields in the Baikal rift zone.

## 2. Geological context: the Baikal pre-rift basement

The evolution of the Baikal pre-rift basement occurred in several major stages, beginning by the formation of the Siberian craton in the Archaean–Early Proterozoic, and followed by the Palaeo-Asian oceanic evolution along its southern margin in the Late Proterozoic–Early Palaeozoic, Palaeo-Mongol–Okhotsk evolution in the Early–Middle Palaeozoic and progressive closure of the Mongol–Okhotsk oceanic gulf in the Late Palaeozoic–Mesozoic (Belichenko et al., 1994; Berzin et al., 1994; Berzin and Dobretsov, 1994; Melnikov et al., 1994). A short review of the existing knowledge on the geodynamic evolution of Central Asia is also presented to integrate the recent developments in this field, not always available to the international scientific community.

### 2.1. The Siberian platform

The Early Precambrian basement of the Siberian platform is mostly concealed under a thick sedimentary cover of Late Proterozoic (Riphean), Early Palaeozoic (Vendian to Early Silurian) and Mesozoic age. In the southern part of the Siberian platform, the Archaean–Early Proterozoic basement outcrops in the Prisayan shield to the southwest, and in the Aldan shield to the southeast (Aftalion et al., 1991; Melnikov, 1991; Rundqvist and Mitrofanov, 1993). In this article, the southeastern half of the Prisayan shield, near Lake Baikal, is described as the Sharyzhalgay complex, according to the Russian terminology.

Consolidation of the basement of the Siberian platform started in the Early Archaean and ended in the Middle–Late Archaean, simultaneously with the development of greenstone and ophiolite belts (Dobretsov et al., 1992). In the Early–Middle Proterozoic, the southeastern margin of the Siberian craton evolved as active continental margin, in association with the development of the Pri-Baikal volcano-plutonic belt (Bukharov, 1973; Neymark et al., 1991).

The present outline of the southern margin of the Siberian platform had a strong influence on the geometry and history of deformations in the adjacent Late Precambrian–Phanerozoic fold belts. It is characterized, from west to east, by the Angara–Lena salient (Angara–Lena plate), the Vitim embayment (Mama–Bodajbo foredeep) and the Aldan shield (Fig. 2).

### 2.2. Riphean continental marginal and initial opening of the Palaeo-Asian ocean

In the Late Proterozoic (Riphean), the southern margin of the Angara–Lena plate evolved into a passive continental margin, with the deposition of terrigenous-carbonaceous sediments in marginal foredeeps, unconformably overlying the volcano-plutonic belt (Baikal series in the Pri-Baikal belt, Bodaibin series in the Baikal–Patom arc), and in the Vitim embayment (Mama–Bodajbo foredeep) (Surkov et al., 1991; Melnikov et al., 1994). This period is believed to mark the initiation of Palaeo-

Asian ocean history in this area (Zonenshain et al., 1990; Dobretsov et al., 1992; Belichenko et al., 1994). The relicts of the oceanic crust are evidenced by Riphean ophiolites (1100–1300 Ma?) in the Baikal–Muya ophiolite belt, north of Lake Baikal (Konnikov, 1991; Dobretsov et al., 1992; Belichenko et al., 1994; Konnikov et al., 1993) and by the Isakian ophiolite belt in the Yenisey ridge (Vernikovskiy et al., 1993). The younger ages for these ophiolites mark the obduction over the passive margin of the Siberian platform, near 650 Ma for the Baikal–Muya belt and at about 600 Ma for the Isakian belt.

### 2.3. Caledonian tectonic collage of microcontinents with the Siberian craton

The Caledonian domain of the Sayan–Baikal fold belt includes a series of Precambrian–Early Palaeozoic composite terranes (or microcontinents) which fringe the Siberian platform: the Khamar Daban–Barguzin (including the Olkhon area), Tuva–Mongolia and Kansk–Derba blocks (Fig. 2). They occurred as archipelagos of large islands of Precambrian basement in the proto-Palaeo-Asian ocean, surrounded by island arcs, back-arc and intra-arc basins (Belichenko et al., 1994; Berzin et al., 1994; Melnikov et al., 1994). Amalgamation of these terranes started in the Vendian. Simultaneously, most of the Siberian platform was covered by marine clastic-carbonate sediments, while the Tuva–Mongolia block was covered by phosphate-bearing carbonates (Ilyin, 1990). Along the southern margin of the Siberian platform, large foredeeps initiated in the Vendian and remained active until the Early Silurian, accumulating up to 5000 m of sediment (Prisayan, Angara–Lena and Kodar–Udokan foredeeps: Melnikov et al., 1994).

Interaction of the Khamar Daban–Barguzin and Tuva–Mongolia blocks with the Siberian platform and the definite closure the oceanic branch between them is believed to have occurred in the Early Palaeozoic (Belichenko et al., 1994; Melnikov et al., 1994). The collision zone is marked, in the Khamar Daban–Barguzin block, by Late Cambrian–Ordovician high-grade metamorphic complexes (Olkhon, Sludyanka), by the intrusion of Late Cambrian–Silurian S-type granites (Angara–Vitim batholith),

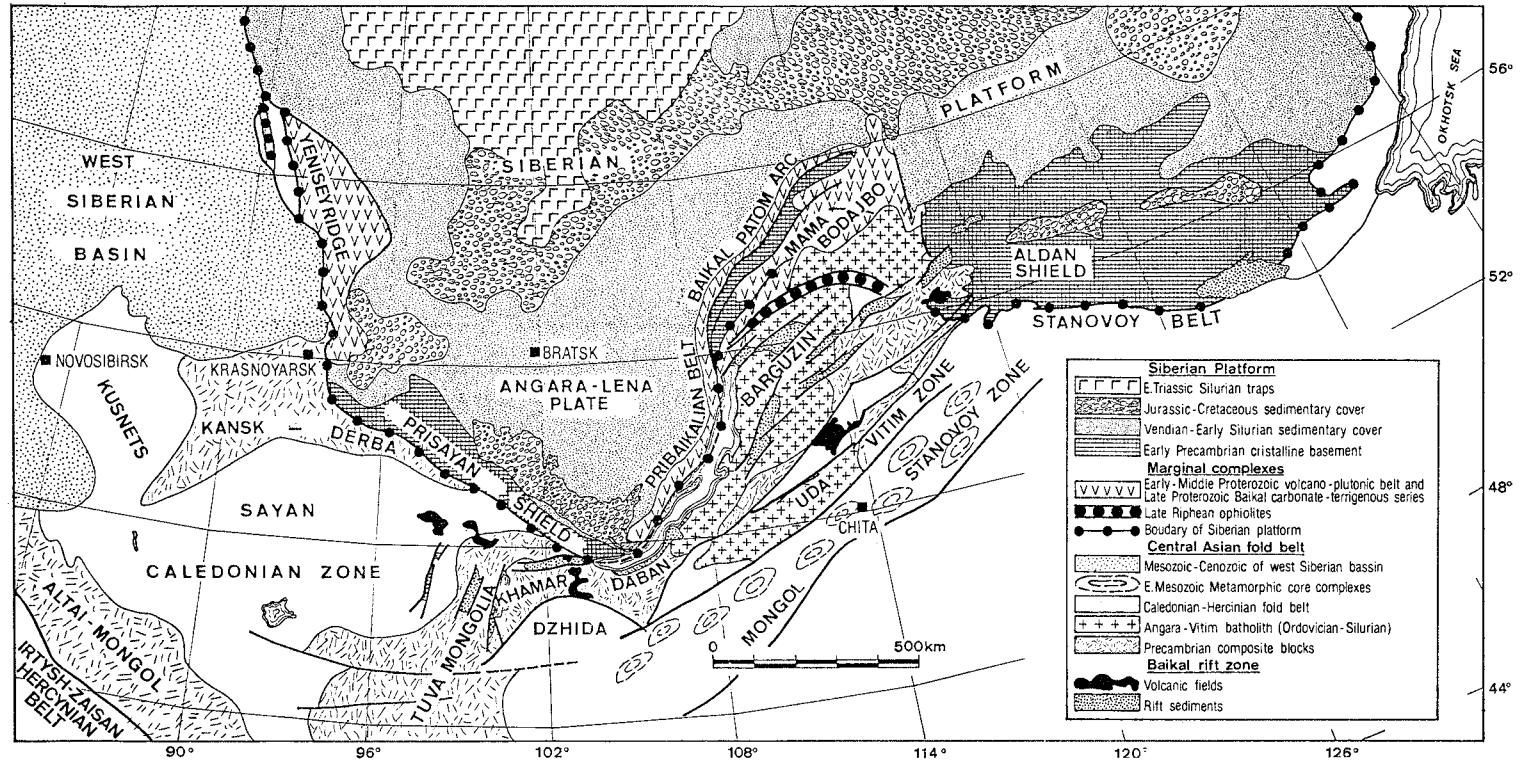


Fig. 2. Tectonic setting of the Pre-Mesozoic basement of the Baikal rift system in Central Asia (redrawn from Belichenko et al., 1994; Berzin et al., 1994; Berzin and Dobretsov, 1994; Melnikov et al., 1994).

and by the intrusion of post-collisional Devonian A-type granites and deposition of Devonian continental molasse (Neymark et al., 1993a, Neymark et al., 1993b). During this long period, two major tectonic events are reported.

The first collision occurred in Early Caledonian times. Between the Tuva–Mongolia microcontinent and the Angara–Lena plate, a branch of the proto-Palaeo-Asian ocean may have existed in the Vendian–Cambrian, with a south-dipping subduction zone beneath the Tuva–Mongolia microcontinent and a passive margin along the southern margin of the Siberian platform (Zorin et al., 1993). The closure of this ocean in the Late Cambrian–Middle Ordovician (*Early Caledonian stage*) resulted in thrusting of the microcontinent over the southern edge of the Siberian platform. In Vendian–Cambrian times, the Khamar Daban–Barguzin microcontinent was already attached to the Siberian platform, as shown by the existence of the Vendian–Cambrian molasse in the Mama–Bodajbo foredeep, and a 600–550 Ma event of metamorphism and granitic magmatism in the Baikal–Muya ophiolite belt (Berzin and Dobretsov, 1994). During the Early Caledonian stage, renewed northwards movement of the Khamar Daban–Barguzin microcontinent relative to the Siberian platform caused lateral reactivation of the suture zone along its western boundary and folding and thrusting of the Riphean sediments of the Mama–Bodajbo foredeep in the Vitim embayment, to the north. An Early Ordovician U–Pb age for this deformation and associated metamorphism in the Vitim embayment was obtained by Bukharov et al. (1992).

After the first collisional stage, the oceanic evolution and subduction migrated southwards, as indicated by the sequence of Vendian–Ordovician thrust sheets with ophiolite fragments in the Dzhida block, south of the junction between the Khamar Daban–Barguzin and Tuva–Mongolia microcontinents (Fig. 2). The Dzhida block may correspond to an external island-arc system that persisted until the Late Ordovician–Silurian (Zorin et al., 1993). This island-arc system marked the initiation of a second stage in the development of the Palaeo-Asian ocean. During this time, sedimentation and subsidence occurred in the marginal foredeeps of the Siberian platform. Now, the Palaeo-Asian ocean is subdivided into two branches by the Tuva–Mongol microcontinent: the

Palaeo-Mongol–Okhotsk branch to the east, and the western Palaeo-Asian ocean to the west.

An abrupt interruption of sedimentation in the marginal foredeeps in the Late Silurian–Early Devonian was associated with a new collisional stage. This *Late Caledonian stage* caused the development of the Pri-Baikal fold-and-thrust belt along the south-eastern margin of the Angara–Lena plate (Alexandrov, 1989). This deformation affects the Early–Middle Proterozoic volcano-plutonic formations, the Riphean Baikal series and the Vendian–Early Ordovician sedimentary cover. Typically, the structure of the northern part of the Pri-Baikal belt is characterized by the successive development of northwest-vergent, low-angle imbricated thrusts, high-angle reverse faults, and younger strike-slip faults (Delvaux et al., 1993). The Late Silurian–Early Devonian age for this tectonic event is indirectly constrained by a stratigraphic gap between Silurian sediments on the Siberian platform and the Middle–Late Devonian molasse which deposited unconformably over the Pri-Baikal and the Sayan–Baikal belts, and Late Silurian–Early Devonian olistostromes in the southeastern Sayan and Dzhida zones (Berzin and Dobretsov, 1994).

After the final Silurian collision, the Caledonian terranes accreted around the southern margin of the Siberian platform (Trans-Baikal area) were partly stabilized. During the Late Palaeozoic, the Trans-Baikal area was affected by crustal extension, post-orogenic magmatism, volcanism and molassic sedimentation in continental basins. The area of orogenic processes and oceanic development migrated south-eastwards, with the ongoing development of the Palaeo-Mongol–Okhotsk branch of the Palaeo-Asian ocean. This may belong to a vast oceanic domain, extending from the Mongol–Okhotsk area to the Polar Urals and consisted of several different oceanic basins, but this matter is still debated (Berzin et al., 1994).

West of the Siberian platform, the Caledonides of the Altai–Sayan area, which result from the Ordovician–Silurian amalgamation, are split in two large massifs, by opening of a new oceanic branch in the Irtysh–Zaisan zone between Kazakhstan and Siberia–Mongolia (Mossakovsky and Dergunov, 1985): the Irtysh–Zaisan branch of the Palaeo-Asian ocean.

#### 2.4. Hercynian closure of the Palaeo-Asian ocean and transition to the Mongol–Okhotsk ocean

The Late Palaeozoic evolution of Central Asia is the consequence of the combined effects of: (1) progressive closure of several branches of the Palaeo-Asian ocean, (2) the Mongol–Okhotsk oceanic evolution in East Asia between the Siberian plate and the Mongol–China plate from the Permian to the Triassic, and (3) general rotation of the Siberian platform together with the stabilized Caledonian rim from the Silurian to the Triassic (Enkin et al., 1992; Sengör et al., 1993; Berzin et al., 1994; Berzin and Dobretsov, 1994; Melnikov et al., 1994). These processes controlled the development of regional strike-slip faults, locally associated to large thrust belts, as in the Kusnets arc and related limnic coal-bearing basins, during the Carboniferous–Permian in the Altai–Sayan area and may also have affected the margin of the Angara–Lena plate and the Trans-Baikal area.

West of the present-day position of the Siberian platform, a Devonian–Carboniferous active continental margin with an oblique subduction zone developed between the Altai–Mongol and Kazakhstan blocks, in the Irtysh–Zaisan zone. A complex collisional history including back-arc rifts, volcano-plutonic belts and accretion prisms has been recognized in the Altai–Mongol margin and adjacent terranes of the Sayan Caledonian zone (Berzin and Dobretsov, 1994):

(1) During the Devonian, one (or possibly two) oblique subduction zone was active at the southwestern margin of the Altai–Mongol block and granitic magmatism occurred in the Altai–Sayan area.

(2) In the Early–Middle Carboniferous, the Devonian ocean was closed by collision of the Kazakhstan and Altai–Mongol blocks, along the Irtysh–Zaisan zone, causing intense dextral strike-slip movements along a 30-km-wide NW-trending blastomylonitic belt in the Irtysh–Zaisan zone and in the adjacent areas.

(3) The Late Carboniferous–Early Permian period was characterized by post-collisional volcano-plutonium in the Altai–Sayan area, with important transcurrent movements along strike-slip faults and limnic sedimentation in fault-related basins. During the same period, collision of the Tien-Shan and

Tarim blocks with the Eurasian continent (Kazakhstan and Siberia) resulted in the final closure of the Irtysh–Zaisan branch of the Palaeo-Asian ocean (Allen et al., 1992; Berzin et al., 1994).

Along the present southern margin of the Khamar Daban–Barguzin block, already attached to the Siberian platform, a northwards-dipping Andean-style subduction zone was active in the Devonian, possibly extending to the Late Jurassic (Enkin et al., 1992; Sengör et al., 1993; Zorin et al., 1993; Belichenko et al., 1994). It is associated with widespread A-type Devonian granite intrusions in the Khamar Daban–Barguzin block, from Mongolia to the Baikal–Patom arc. This Devonian subduction zone marks the southern limit of the Mongol–Okhotsk ocean. Also in the Devonian, a possible dextral translation of the Mongol–Okhotsk ocean relative to the Siberian continent occurred (Sengör et al., 1993).

Starting in the Late Carboniferous, the new phase of extensional tectonism along this zone marks the beginning of the history of the Mongol–Okhotsk ocean, which perdured in the Permian, until the end of the Jurassic. The Palaeozoic–Mesozoic transition is marked by the development of a narrow NE-trending belt of metamorphic core complexes in the Trans-Baikal area, extending from Mongolia to the Stanovoy belt (Sklyarov, 1993). Formation of these complexes in the studied area probably occurred in the Late Permian–Early Triassic. They are associated to post-orogenic volcano-plutonium and can be regarded as indicators of extensional tectonism of a Cordilleran-type.

#### 2.5. Mesozoic closure of the Mongol–Okhotsk ocean

The Mesozoic period is characterized by the continuation of oceanic evolution in the eastern part of the Mongol–Okhotsk ocean and its final closure in the Late Jurassic–Early Cretaceous, as the consequence of the lithospheric collision of Eurasia (Siberia and Kazakhstan) with a series of microcontinents already assembled into the Mongolia–China block (Khain, 1990; Enkin et al., 1992; Belichenko et al., 1994). Deformation was not confined to the collisional zone, but spread over the Caledonian–Hercynian continental area, reaching the margin of the Siberian platform in the Trans-Baikal area (Ermikov, 1994).

After a Mid-Triassic unconformity, the Mesozoic activity in Trans-Baikal involves granitoid intrusion, volcanism with coal-bearing limnic sedimentation and differential uplifting. Along the margin of the Siberian platform, large foredeeps accumulated coal-bearing molasses in the Early–Middle Jurassic.

In the Trans-Baikal area, intense vertical movements in the Late Triassic mark the initiation of tectonically induced chains of shallow basins, separated by uplifted basement blocks. They develop as a series of narrow basins along en-echelon zones, reactivating major crustal faults. They can be either symmetrical or asymmetrical, filled by Late Triassic volcanics, Early–Middle Jurassic volcano-sedimentary molasse, Late Jurassic–Early Cretaceous coal-bearing limnic sediments and Middle Cretaceous conglomerates and breccias. The Trans-Baikal Mesozoic basins are generally believed to initiate in a general extensive context, following the development of metamorphic core complexes (Sklyarov, 1993). The Late Triassic volcanic period probably corresponds to this initial extension. The Late Jurassic–Early Cretaceous coal-bearing limnic sedimentation may already be related to a transpressive environment. From the end of the Early Cretaceous to the Late Cretaceous, mega-breccias, conglomerates, and trachy-basalts were deposited with a gentle unconformity over the Early Cretaceous coal-bearing beds of the Trans-Baikal basins. These are clearly related to later thrust movements along major border faults, causing the partial closure of the basins (Soloviev, 1968; Ermikov, 1994). This points to the existence of a tectonic inversion, probably in the Late Jurassic, after a probable initial extension with deposition of the Early–Middle Jurassic volcano-sedimentary molasse.

On the southern margin of the Siberian platform, Early–Middle Jurassic continental molasses deposited in several large foredeep basins: the Prisayan–Angara and the Pristanovoy basins, both developed in front of south-dipping faults (Ermikov, 1994). The Prisayan–Angara fault was clearly active during sedimentation, but the type of fault (normal or reverse) is not clear for this period. Late Mesozoic reverse movements along this fault caused thrusting of the basement of the Siberian Platform rim (the Sharyzhgaysk complex), over the Middle Jurassic molasse.

In the Late Cretaceous–Palaeogene, a long period of tectonic quietness marks the transition between the Palaeozoic–Mesozoic pre-rift period and the Cenozoic rifting period. It caused an extensive peneplanation over most of Central Asia, with development of kaolinite soil and laterite crust in a warm humid climate. Thin lignite-bearing formations derived from weathering products were deposited in shallow depressions in the Baikal and Trans-Baikal area (Logatchev, 1993; Ermikov, 1994; Kashik and Mazilov, 1994).

### 3. Structural analysis and palaeostress reconstruction

Field investigation of fault kinematics was conducted along the whole western coast of Lake Baikal, in the Pri-Baikal belt, and in the Trans-Baikal area, southeast of the lake. Palaeostress tensors were obtained by the application of a stress inversion technique on fault measurements. The results are presented separately for four geographic provinces, and the relative chronology of the palaeostress stages are established when possible. The parameters of the stress tensors are presented in Table 1. In the next sections, the tectonic implications will be examined and the results will be integrated in the regional geodynamic evolution of Central Asia.

#### 3.1. Stress inversion method

Fault plane and slip line orientations, including slip senses are used to compute the four parameters of the reduced stress tensor, as defined in Angelier (1989; Angelier, 1991a): the principal stress axes  $\sigma_1$  (maximum compression),  $\sigma_2$  (intermediate compression) and  $\sigma_3$  (minimum compression) and the ratio of principal stress differences  $R = (\sigma_2 - \sigma_3) / (\sigma_1 - \sigma_3)$ . The two additional parameters of the full stress tensor are the ratio of extreme principal stress magnitudes ( $\sigma_3 / \sigma_1$ ) and the lithostatic load, but these cannot be determined from fault data only. The first four parameters are determined using successively an improved version of the Right Dihedron method of Angelier and Mechler (1977), and a rotational optimization method, using the TENSOR computer program developed by Delvaux (1993).

Table 1

Parameters of the reduced stress tensors computed for the four pre-Cenozoic palaeostress stages in the Baikal area

| <b>Palaeozoic stage 1 (N–S compression, in brittle–ductile conditions)</b>  |                                   |          |         |            |            |            |          |            |                          |
|---|-----------------------------------|----------|---------|------------|------------|------------|----------|------------|--------------------------|
| <i>Pri-Olkhon area: semi-ductile shear deformation (mylonitic planes and mineral extension lineations)</i>                              |                                   |          |         |            |            |            |          |            |                          |
| Site  | Area/Stratigraphy/Structure       | <i>n</i> | %/total | $\sigma_1$ | $\sigma_2$ | $\sigma_3$ | <i>R</i> | $\alpha$   | Tensor type              |
| Area SW of Birchim massif (+)   |                                   | 34       | 100     | 27/163     | 25/059     | 52/294     | 0.52     | 7.4        | pure compressive         |
| Area NE of Birchim massif (+)   |                                   | 31       | 100     | 05/010     | 80/132     | 08/279     | 0.38     | 11.3       | pure strike-slip         |
| (+ ) mylonitic planes used as movement planes and mineral lineation assumed as indicator of maximum shear directions.                   |                                   |          |         |            |            |            |          |            |                          |
| <i>Pri-Olkhon area: brittle deformation around the Birchim gabbro–syenite intrusion</i>   |                                   |          |         |            |            |            |          |            |                          |
| Site  | Area/Stratigraphy/Structure       | <i>n</i> | %/total | $\sigma_1$ | $\sigma_2$ | $\sigma_3$ | <i>R</i> | $\alpha$   | Tensor type              |
| BA071   | Kedrovoy cape                     | 25       | 46 *    | 07/355     | 82/147     | 04/264     | 0.15     | 11.3       | compressive strike-slip  |
| BA084   | Zunduk River, marble              | 20       | 71 *    | 12/174     | 12/081     | 73/308     | 0.62     | 13.0       | pure compressive         |
| BA083   | Zunduk lake shore, marble         | 16       | 71      | 09/162     | 09/070     | 78/296     | 0.11     | 7.1        | strike-slip compressive  |
| BA049   | Olkhon Gate, Olkhon gneiss        | 34       | 42 **   | 17/162     | 03/252     | 73/349     | 0.65     | 10.5       | pure compressive         |
| BA051   | Olkhon Gate, Olkhon gneiss        | 14       | 50 *    | 11/178     | 11/270     | 74/046     | 0.79     | 10.1       | pure compressive         |
| BA052   | Olkhon Gate, Olkhon gneiss        | 8        | 22 *    | 01/160     | 05/251     | 85/058     | 0.38     | 10.1       | pure compressive         |
| BA068   | Baikal shore, pegmatite dyke      | 6        | 13 **   | 26/224     | 61/015     | 12/128     | 0.15     | 3.8        | compressive strike-slip  |
| BA067   | Anga Bay, marble                  | 8        | 32 *    | 05/254     | 77/141     | 12/346     | 0.43     | 4.2        | pure strike-slip         |
| id.   |                                   | 11       | 44 *    | 04/219     | 08/309     | 81/105     | 0.67     | 9.5        | pure compressive         |
| BA034   | Buguldeyka, unsheared granite     | 9        | 41 *    | 02/349     | 01/259     | 88/131     | 0.34     | 5.4        | pure compressive         |
| BA030   | Kuyada Bay, dioritic gneiss       | 15       | 30 *    | 02/190     | 05/100     | 85/302     | 0.06     | 11.6       | compressive strike-slip  |
| id.   |                                   | 10       | 20 *    | 13/010     | 75/222     | 08/102     | 0.41     | 7.9        | pure strike-slip         |
| Weighed mean: 10 tensors<br>(Ba067 and Ba068 excluded)  |                                   | 164      |         | 06/171     | 06/262     | 82/035     | 0.31     |            | pure compressive         |
| <b>Palaeozoic stage 2 (NW–SE compression)</b>   |                                   |          |         |            |            |            |          |            |                          |
| <i>North Baikal: Pri-Baikal fold and thrust belt, Early–Middle Proterozoic Akitkan volcano-plutonic group, lower greenschist facies</i> |                                   |          |         |            |            |            |          |            |                          |
| Site  | Area/Stratigraphy/Structure       | <i>n</i> | %/total | $\sigma_1$ | $\sigma_2$ | $\sigma_3$ | <i>R</i> | $\alpha$   | Tensor type              |
| BA076   | Kotelnikoskiy, low-angle thrust   | 30       | 68      | 12/117     | 01/022     | 78/292     | 0.49     | 9.7        | pure compressive         |
| BA075   | Muzhinai (poorly constrained)     | 5        | 62      | 11/123     | 06/031     | 78/271     | 0.91     | 2.6        | radial compressive       |
| BA080   | Kosa cape, thrust zone            | 19       | 30 **   | 04/307     | 22/038     | 69/205     | 0.95     | 9.0        | radial compressive       |
| BA081   | Malaya Kosa cape, thrust zone     | 23       | 79      | 03/122     | 16/031     | 74/222     | 0.91     | 13.5       | radial compressive       |
| BA082   | Khibelen cape, reverse fault      | 28       | 80      | 13/046     | 09/314     | 74/189     | 0.92     | 11.5       | radial compressive       |
| BA074   | Elochyn cape                      | 9        | 82      | 08/161     | 35/256     | 54/060     | 0.27     | 9.0        | pure compressive         |
| Weighed mean: 6 tensors   |                                   | 114      |         | 02/125     | 05/035     | 85/237     | 0.75     |            | near-radial compressive  |
| <i>Central Baikal: Primorsky dislocation zone, Olkhon complex</i>   |                                   |          |         |            |            |            |          |            |                          |
| Site  | Area/Stratigraphy/Structure       | <i>n</i> | %/total | $\sigma_1$ | $\sigma_2$ | $\sigma_3$ | <i>R</i> | $\alpha$   | Tensor type              |
| BA052   | Olkhon gate                       | 22       | 59 *    | 03/308     | 17/217     | 73/047     | 0.10     | 11.2       | strike-slip compressive  |
| BA068   | Pri-Olkhon, affect pegmatite dyke | 14       | 30 **   | 03/324     | 82/217     | 08/054     | 0.10     | 12.2       | compressive. strike-slip |
| BA050   | Elansi, Anga River                | 19       | 66      | 13/306     | 71/177     | 15/039     | 0.65     | 7.1        | pure strike-slip         |
| BA046   | Cape Goliy, diorite intrusion     | 14       | 70      | 05/338     | 84/194     | 03/068     | 0.36     | 7.3        | pure strike-slip         |
| BA034   | Buguldeika, rapakivi granite      | 6        | 27 *    | 29/296     | 24/040     | 52/163     | 0.28     | 8.6        | pure compressive         |
| BA005   | Buguldeika, Baikal shore          | 25       | 47 *    | 15/322     | 06/054     | 74/163     | 0.15     | 12.0       | strike-slip compressive  |
| BA036   | Kurtun, E. Prot. rapakivi granite | 13       | 72      | 04/117     | 10/027     | 80/229     | 0.06     | 12.8       | strike-slip compressive  |
| BA038   | Riph. dolom., fracture cleavage   | 27       | 100     | 15/295     | 12/028     | 71/155     | 0.10     | $\sigma_N$ | strike-slip compressive  |
| id.   | Riph. shale, conjug. shear planes | 17       | 100     | 01/134     | 06/224     | 84/033     |          | $\sigma_T$ | compressive              |
| BA039   | Buguldeika, Primorsky zone        | 33       | 69 *    | 22/293     | 69/092     | 07/201     | 0.08     | 14.3       | compressive strike-slip  |
| Weighed mean: 11 tensors  |                                   | 190      |         | 09/312     | 80/151     | 03/042     | 0.04     |            | compressive strike-slip  |

Table 1 (continued)

| <i>South Baikal: Sharyzhalgay block–Main Sayan dislocation</i> |                                  |          |         |            |            |            |          |          |                         |
|--|----------------------------------|----------|---------|------------|------------|------------|----------|----------|-------------------------|
| Site   | Area/Stratigraphy/Structure      | <i>n</i> | %/total | $\sigma 1$ | $\sigma 2$ | $\sigma 3$ | <i>R</i> | $\alpha$ | Tensor type             |
| BA002  | Sharyzhalgay, Lystvianka         | 8        | 89      | 30/142     | 60/324     | 01/233     | 0.28     | 9.0      | compressive strike-slip |
| BA100  | Sharyzhalgay, Lystvianka         | 35       | 31 * *  | 09/309     | 57/205     | 31/044     | 0.12     | 13.3     | pure strike-slip        |
| BA103  | Sharyzhal., pre 296–321 Ma dykes | 21       | 26 *    | 02/139     | 24/229     | 66/044     | 0.20     | 8.4      | strike-slip compressive |
| BA016  | Sharyzhalgay, railway km 140     | 25       | 42 *    | 02/299     | 07/029     | 81/191     | 0.20     | 10.3     | strike-slip compressive |
| BA023  | Main Sayan fault, Irkut River    | 18       | 37 *    | 10/292     | 80/108     | 10/202     | 0.48     | 11.4     | pure strike-slip        |
| Weighed mean: 5 tensors  |                                  | 107      |         | 02/129     | 88/291     | 01/039     | 0.05     |          | compressive strike-slip |

**Palaeozoic stage 3 (E–W compression)***North Baikal: Pri-Baikal fold-and-thrust belt*

| Site                    | Area/Stratigraphy/Structure | <i>n</i> | %/total | $\sigma 1$ | $\sigma 2$ | $\sigma 3$ | <i>R</i> | $\alpha$ | Tensor type             |
|-------------------------|-----------------------------|----------|---------|------------|------------|------------|----------|----------|-------------------------|
| BA080                   | Kosa cape                   | 17       | 27 * *  | 11/282     | 63/034     | 25/187     | 0.20     | 13.7     | compressive strike-slip |
| BA073                   | Elochin strike-slip fault   | 19       | 46 *    | 13/279     | 58/167     | 29/016     | 0.42     | 11.0     | pure strike-slip        |
| Weighed mean: 2 tensors |                             | 36       |         | 12/281     | 78/112     | 02/011     | 0.31     |          | pure strike-slip        |

*Central Baikal: Primorsky dislocation, Olkhon complex*

| Site                    | Area/Stratigraphy/Structure       | <i>n</i> | %/total | $\sigma 1$ | $\sigma 2$ | $\sigma 3$ | <i>R</i> | $\alpha$ | Tensor type             |
|-------------------------|-----------------------------------|----------|---------|------------|------------|------------|----------|----------|-------------------------|
| BA049                   | Olkhon Gate                       | 23       | 28 * *  | 04/081     | 85/247     | 01/351     | 0.92     | 11.3     | extensive strike-slip   |
| BA049                   | Olkhon Gate                       | 16       | 20 * *  | 08/275     | 17/183     | 72/028     | 0.14     | 12.8     | strike-slip compressive |
| BA068                   | Pri-Oikhon, affect pegmatite dyke | 16       | 34 * *  | 09/282     | 09/191     | 77/057     | 0.40     | 9.9      | pure compressive        |
| BA045                   | Cape Goliy, thrust system         | 21       | 68      | 29/086     | 07/352     | 60/249     | 0.57     | 8.5      | pure compressive        |
| Weighed mean: 4 tensors |                                   | 76       |         | 04/091     | 84/316     | 04/181     | 0.01     |          | compressive strike-slip |

*South Baikal: Sharyzhalgay block–Main Sayan dislocation*

| Site                                   | Area/Stratigraphy/Structure         | <i>n</i> | %/total | $\sigma 1$ | $\sigma 2$ | $\sigma 3$ | <i>R</i> | $\alpha$   | Tensor type                  |
|--|-------------------------------------|----------|---------|------------|------------|------------|----------|------------|------------------------------|
| Sharyzhalgay 296–331 Ma dykes (dieder) |                                     |          |         |            |            |            |          |            |                              |
|  |                                     | 12       | 100     | 03/279     | 84/156     | 05/009     | 1.00     | $\sigma N$ | extensive strike-slip<br>min |
| BA100                                  | Sharyzhalgay, Lystvianka            | 13       | 12 *    | 09/075     | 10/167     | 77/303     | 0.49     | 7.3        | pure compressive             |
| BA104                                  | Sharyzhalgay                        | 6        | 18 *    | 13/284     | 70/055     | 14/190     | 0.61     | 7.7        | pure strike-slip             |
| BA105                                  | Sharyzhalgay, Maritui               | 52       | 69 * *  | 01/098     | 05/188     | 85/353     | 0.48     | 13.6       | pure compressive             |
| id.                                    |                                     | 8        | 11 * *  | 04/086     | 35/178     | 54/350     | 0.46     | 4.1        | oblique compressive          |
| BA015                                  | Sharyzhalgay, railway km 169        | 15       | 37 *    | 06/076     | 08/167     | 80/314     | 0.89     | 9.1        | semi-radial compressive      |
| id.                                    |                                     | 18       | 45 *    | 16/063     | 74/239     | 01/332     | 0.05     | 9.8        | compressive strike-slip      |
| BA016                                  | Sharyzhalgay, railway km 140        | 15       | 25 *    | 03/084     | 80/190     | 10/353     | 0.27     | 3.6        | pure strike-slip             |
| BA107                                  | Sharyzhalgay, brittle–ductile fault | 18       | 54      | 08/085     | 19/353     | 70/197     | 0.43     | 9.7        | pure compressive             |
| Weighed mean: 9 tensors                |                                     | 157      |         | 03/087     | 12/178     | 77/343     | 0.23     |            | strike-slip compressive      |

**Mesozoic (N–S compression, in superficial conditions)***Sharyzhalgay block, Angara thrust*

| Site                    | Area/Stratigraphy/Structure      | <i>n</i> | %/total | $\sigma 1$ | $\sigma 2$ | $\sigma 3$ | <i>R</i> | $\alpha$ | Tensor type              |
|-------------------------|----------------------------------|----------|---------|------------|------------|------------|----------|----------|--------------------------|
| BA003                   | Archaean/Jurassic Angara thrust  | 13       | 68      | 11/014     | 02/105     | 79/204     | 0.19     | 7.1      | strike-slip compressive. |
| BA023                   | Main Sayan fault zone            | 18       | 37 *    | 29/353     | 60/161     | 05/260     | 0.45     | 11.7     | pure strike-slip         |
| BA100                   | Archaean, near Angara thrust     | 34       | 30 * *  | 07/184     | 04/274     | 82/034     | 0.45     | 9.9      | pure compressive         |
| BA101                   | Jurassic: slip on bedding planes | 15       | 54      | (68/043    | 11/281     | 18/187     | 0.68     | 13.3     | oblique extensive        |
| BA102                   | Archaean, incohesive breccia     | 15       | 71 *    | 12/028     | 70/155     | 15/295     | 0.57     | 8.8      | pure strike-slip         |
| BA103                   | Archaean, post 296–321 Ma dykes  | 46       | 57 *    | 04/202     | 00/111     | 86/020     | 0.35     | 9.4      | pure compressive         |
| BA104                   | Archaean, incohesive breccia     | 15       | 50 *    | 11/186     | 06/277     | 77/035     | 0.33     | 8.5      | pure compressive         |
| BA105                   | Archaean, incohesive breccia     | 8        | 11 * *  | 17/001     | 50/113     | 34/258     | 0.67     | 7.7      | oblique strike-slip      |
| Weighed mean: 8 tensors |                                  | 164      |         | 07/010     | 09/279     | 78/137     | 0.11     |          | strike-slip compressive  |

Table 1 (continued)

| <i>Selenga–Itantsy rivers: Posolsky fault</i> |                                  |          |         |            |            |            |          |          |                       |
|---|----------------------------------|----------|---------|------------|------------|------------|----------|----------|-----------------------|
| Site  | Area/Stratigraphy/Structure      | <i>n</i> | %/total | $\sigma_1$ | $\sigma_2$ | $\sigma_3$ | <i>R</i> | $\alpha$ | Tensor type           |
| BA113   | Early Proterozoic Diorite        | 18       | 37 *    | 14/205     | 02/114     | 76/019     | 0.57     | 10.1     | pure compressive      |
| id.   |                                  | 18       | 37 *    | 24/020     | 03/111     | 66/206     | 0.58     | 8.0      | pure compressive      |
| BA114   | Cretaceous overlain by Pliocene  | 16       | 62      | (80/062)   | 01/159     | 09/250     | 0.49     | 6.8      | pure extensive        |
| BA115   | Cambrian thrust on E. Prot.      | 30       | 61 *    | 03/346     | 04/256     | 85/107     | 0.55     | 9.4      | pure strike-slip      |
| id.   | (epidote on fault planes)        | 10       | 20 *    | 24/132     | 03/040     | 66/301     | 0.50     | 8.6      | pure compressive      |
| BA126   | Faults cutting dykes (epidote)   | 22       | 58      | 10/170     | 19/263     | 68/057     | 0.78     | 9.3      | pure compressive      |
| Weighed mean: 6 tensors                       |                                  | 114      |         | 05/175     | 04/263     | 87/349     | 0.27     |          | pure compressive      |
| <i>Uda–Gusinoye depression</i>                |                                  |          |         |            |            |            |          |          |                       |
| Site  | Area/Stratigraphy/Structure      | <i>n</i> | %/total | $\sigma_1$ | $\sigma_2$ | $\sigma_3$ | <i>R</i> | $\alpha$ | Tensor type           |
| BA109   | Late Palaeozoic granite          | 12       | 55 *    | 03/357     | 79/101     | 10/268     | 0.36     | 7.4      | pure strike-slip      |
| BA110   | Late Palaeozoic granite          | 10       | 50      | 03/350     | 87/169     | 00/080     | 0.15     | 5.6      | compressive strike-s  |
| BA116   | U. Prot. sheared granite         | 21       | 78      | 16/185     | 02/276     | 74/012     | 0.22     | 8.6      | strike-slip compressi |
| BA117   | U. Palaeozoic granite (epidote)  | 34       | 77      | 12/016     | 10/284     | 74/154     | 0.08     | 12.1     | strike-slip compressi |
| BA118   | Late Palaeozoic granite          | 15       | 75      | 03/352     | 21/261     | 68/090     | 0.11     | 6.3      | strike-slip compressi |
| BA120   | E-Cret., lava injected in thrust | 6        | 100     | 01/006     | 11/176     | 79/101     | 0.57     | 4.9      | pure compressive      |
| BA124   | E–M Jurassic andesite lava       | 20(o)    | 42 *    | 12/201     | 13/109     | 72/332     | 0.53     | 9.8      | pure compressive      |
| id.   |                                  | 17(y)    | 35 *    | 04/133     | 38/040     | 52/228     | 0.18     | 8.8      | strike-slip compressi |
| Weighed mean: 8 tensors                       |                                  | 135      |         | 01/178     | 02/268     | 87/065     | 0.15     |          | strike-slip compressi |
| <i>Tugnui depression</i>                      |                                  |          |         |            |            |            |          |          |                       |
| Site  | Area/Stratigraphy/Structure      | <i>n</i> | %/total | $\sigma_1$ | $\sigma_2$ | $\sigma_3$ | <i>R</i> | $\alpha$ | Tensor type           |
| BA112   | E. Prot. thrust on E-Cret.       | 29       | 69      | 17/206     | 02/115     | 73/018     | 0.03     | 10.9     | strike-slip compressi |

*n* = total number of data; %/total = percentage of data used for computation;  $\sigma_1$ ,  $\sigma_2$  and  $\sigma_3$  = principal stress directions in forma dip/azimuth; *R* = principal stress ratio  $(\sigma_2 - \sigma_3)/(\sigma_1 - \sigma_3)$ ;  $\alpha$  = mean deviation angle between observed and computed slip directions tensor type is given according to the definition in Fig. 3. In general, the parameters refer to stress tensors obtained by minimization of  $\alpha$  angles for fault planes with slip lines. Some tensors were also obtained by maximization of normal stress magnitudes ( $\sigma_N$  max, for compression joints), maximization of shear stress magnitudes ( $\sigma_T$  max, for conjugated shear joints) or minimization of normal stress magnitudes ( $\sigma_N$  min, for tension joints). In the case of multiple tensor determination of the same site, \* refers to a two-stage population and \*\* refers to a three-stage population.

During the rotational optimization, different functions can be optimized according to the nature of tectonic structure used. For faults, the angular deviation between observed slip lines and computed shears is minimized, together with the maximization of friction coefficients for each fault plane. Not only fault planes with slip lines can be used for the reconstruction of stress tensors, but also tension and compression structures (Angelier, 1991b). Quartz veins, plume joints and dykes are considered as tension joints, developing perpendicular to the least compressive stress axis ( $\sigma_3$ ) and fracture cleavages are considered as compression joints, developing perpendicular to the maximum compressive stress

axis ( $\sigma_1$ ). For them, the resolved normal stress magnitude is respectively minimized and maximized

The TENSOR procedure optimizes the appropriate function by progressive rotation of the tensor around each of his axes, and by testing different values of *R*. The amplitude of rotation angle and values of *R* ratio tested are progressively reduced, until the tensor is stabilized. Separation of fault populations resulting from successive tectonic regimes are based on interactive kinematic separation and progressive stress tensor optimization, to obtain homogeneous subsets, representing different stress regimes. Their chronological succession is established as a function of microstructural and geolog

ical criteria and in relation with known regional tectonic events.

Regional evolution of the stress field is shown on structural maps by symbols indicating, as in Guiraud et al. (1989), the directions of the two horizontal stress axes ( $S_{Hmax}$  and  $S_{Hmin}$ ), with black inward arrows for compressive deviatoric stress and white outward arrows for extensive deviatoric stress, and their length according to the relative stress magnitude in function of the stress ratio  $R$ . The vertical axis is symbolized as an open circle for a compressive regime (vertical extension), a dot for a strike-slip regime and a black circle for an extensive regime (vertical compression). The stress tensors are classified into: *radial / pure / strike-slip extensive*, *extensive / pure / compressive strike-slip* or *strike-slip / pure / radial compressive*, as a function of the relative magnitude of the intermediate axis, given by the stress ratio  $R$  (Fig. 3).

The computed stress tensors are models of homogeneous stress states which are consistent with the observed data, as a function of a series of basic assumptions (Pollard et al., 1993). The first basic assumption is that the slip occurs in the direction of the maximum resolved shear stress on the fault plane (Bott, 1959). The slip apparent direction on the fault is inferred from frictional grooves or slickenlines. The first assumption implies that movement on faults occurs independently of each other. Additional assumptions are that the failure criterion is verified for each neofomed fault and that the friction criterion is also verified for each reactivated pre-existing discontinuity ('initial friction law' of Jaeger, 1969). The fault population should also belong to a single stress regime.

In practice, these assumptions are never strictly verified and reasonable approximations are made. Complications may arise for one or several reasons:

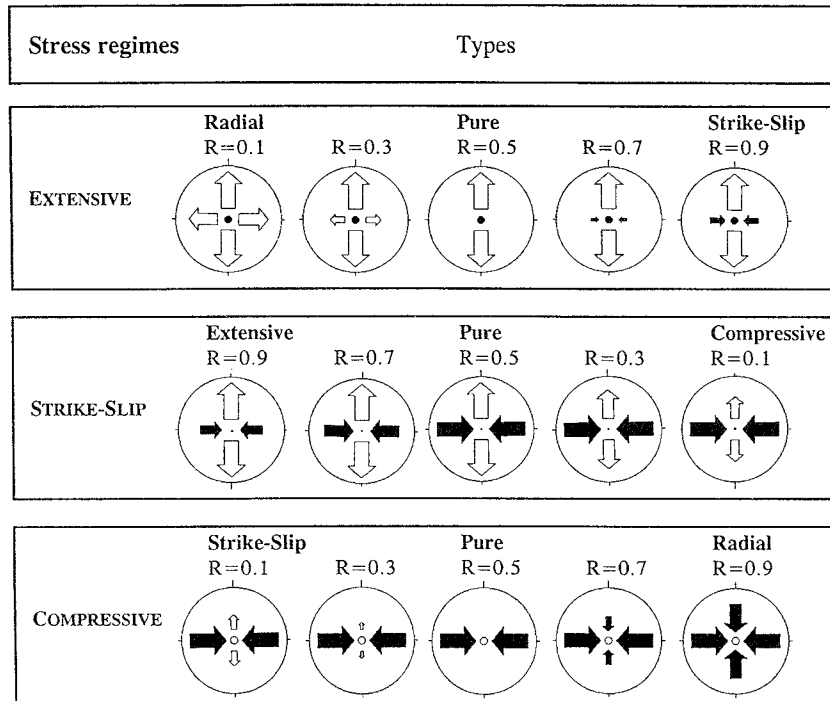


Fig. 3. Types of stress regimes and their representation in map view. Arrows indicate the azimuth of horizontal stress axes, with their length according to the relative stress magnitude, in function of the stress ratio  $R$ . White outward arrows indicate extensive deviatoric stress axes and black inward arrows indicate compressive deviatoric stress axes. Vertical stress axes are symbolized by a solid circle for extensive regimes ( $\sigma_1$  vertical), a dot for strike-slip regimes ( $\sigma_2$  vertical) or an empty circle for compressive regimes ( $\sigma_3$  vertical).

the failure and friction criteria are incompletely known, local stress deviations are caused by non-independent slip on faults (Dupin et al., 1993; Pollard et al., 1993), local rotation of rock fragments may occur inside the observed faulted block, and the stress regime may change during time (polyphase evolution). In consequence, separation of total fault populations into homogeneous subsets is often necessary. The best solution for each subset will be the tensor that gives the lowest mean angular deviation between the observed slips and theoretical shears, and the highest friction angle (or shear stress magnitude) for a maximum number of faults.

These factors are reflected in the common observation that relatively large distributions of deviation angles between observed and computed slips are generally obtained in stress inversion (up to 30°, with a mean deviation of 10°). Critical evaluations by Dupin et al. (1993) and Pollard et al. (1993) indicate that the angular discrepancies are generally in the range of measurement errors and that the influence on the final result is limited. However, for regional reconstructions of stress fields, the possible discrepancies between the computed local stress tensors and the regional stress tensor implies the need for a large number of observation sites.

### 3.2. North Baikal: Pri-Baikal fold-and-thrust belt

Detailed investigation of the northern part of the Pri-Baikal belt indicates the existence of three distinct Proterozoic complexes, differentiated in their age and composition and separated by clear tectonic unconformities (Alexandrov, 1989; Delvaux et al., 1993). The general structure of this area is characterized by the successive development of low-angle thrusts, high-angle reverse faults and later strike-slip faults. In addition, the high-angle reverse faults were reactivated as normal faults during Cenozoic extension.

Early Proterozoic formations were thrust over Middle and Late Proterozoic series along low-angle faults. The best example comes from the right bank of the Khibelen River, where a low-angle fault cuts the overturned flank of a recumbent syncline, separating Early and Middle Proterozoic rocks (Delvaux et al., 1993). The base of the thrust sheet is characterized by strongly deformed plagiogranites, which evolved into banded mylonitic schists. Microstruc-

tural and textural observations indicate that the thrust sheet has been transported to the northwest in a N300°E direction, in modern coordinates. The geographical extent of the remnants of the allochthonous Early Proterozoic suggests that they belong to a large thrust sheet, rooted in the basement of the actual Baikal depression and moving to the northwest. In the adjacent Siberian platform, geological mapping indicated that the 3000-m-thick Riphean–Cambrian cover is deformed in linear NE-striking asymmetric folds, with 50–70° SE-dipping axial planes and regularly affected by thrust and reverse faults. Geophysical exploration demonstrated the existence of horizontal decollement zones in the middle part of the Riphean complex at a depth of 1000–2000 m (Fig. 4b, section A–A'). A major decollement separates the surficial thin-skinned nappe structure involving the Late Riphean, from the Precambrian basement and its subhorizontal Early Riphean cover (Alexandrov, 1989; Melnikov et al., 1994).

A series of NE-trending, SE-dipping high-angle reverse faults, running parallel to the Baikal shore, cut and displace the low-angle thrust faults. They can be followed over tens of kilometres and are associated with a cataclastic zone (maximum thickness 30 m). In addition, high-angle strike-slip faults affect the whole structure, as for example, the left-lateral Elokhin strike-slip fault, striking WNW–ESE, across the general trend of the Pri-Baikal belt (Delvaux et al., 1993). This fault is associated to a conjugate right-lateral fault of NNE–SSW trend, indicating a development under E–W-oriented principal compression.

The palaeostress tensors obtained for this area are listed in Table 1 and displayed on the structural maps of Fig. 4b and 4c. Selected examples are shown in Fig. 5. They are grouped according to their similarities as a function of stress regime and stress axis orientation, and classified chronologically according to the above structural relations. In the general reconstruction they are reported to Palaeozoic stages 2 and 3.

The first stage observed in the North Baikal area is characterized by a compressive regime, intermediate between a pure compression and a radial compression (Fig. 4b). The principal compression axis ( $\sigma_1$ ) is horizontal, with a NW–SE orientation (N125–305°E), and the principal extension axis ( $\sigma_3$ )

is subvertical. This regime corresponds mainly to the development of high-angle reverse faults (e.g., site 80(1), Fig. 5) and low-angle thrusts (e.g., site 76a,

Fig. 5). This principal direction of compression correlates well with the direction of tectonic transport of the thrust nappes (N300°E).

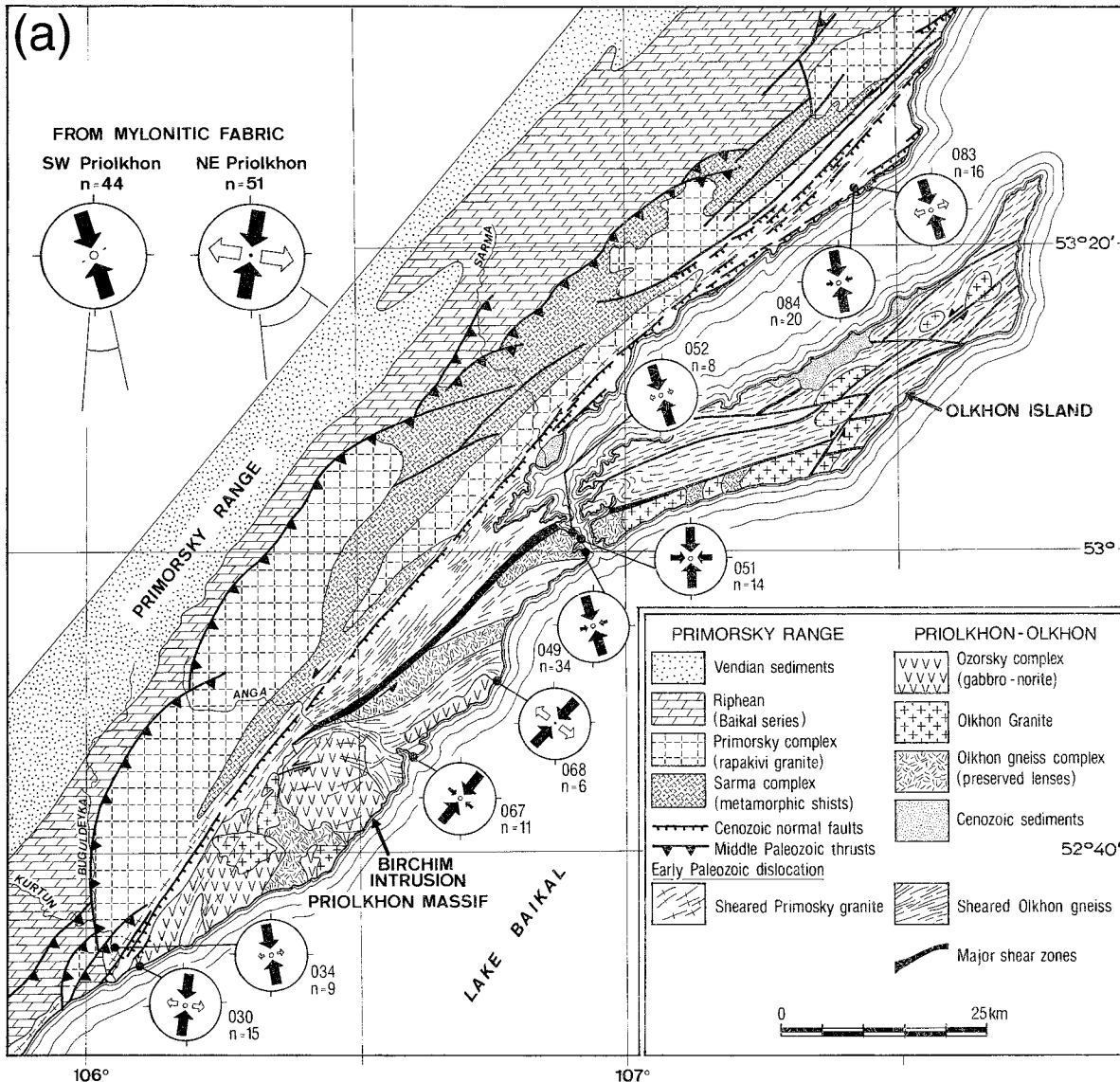
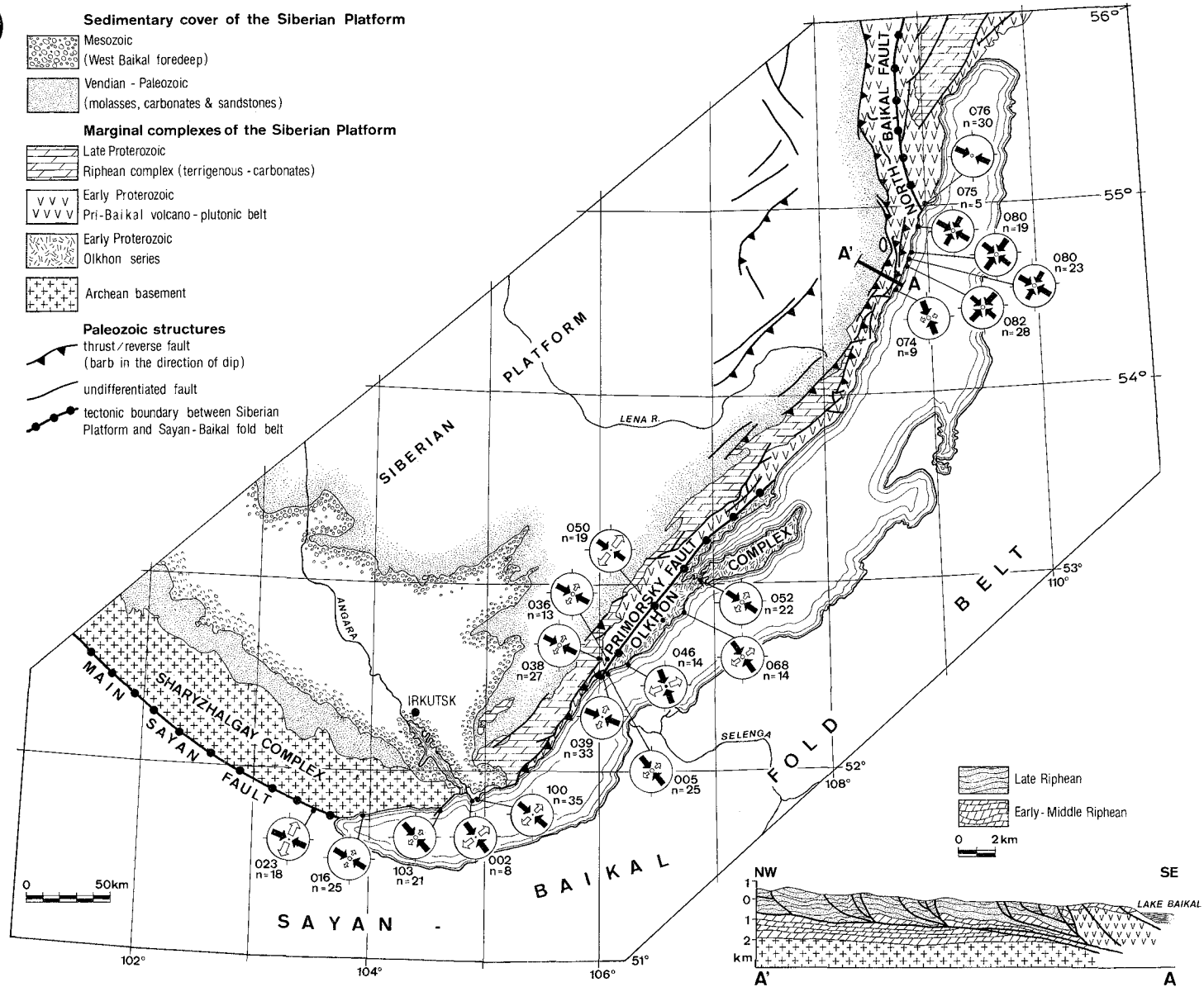


Fig. 4. Structural map with palaeostress symbols as in Fig. 3. Small numbers refer to outcrop number (parameters in Table 1), and to the quantity of data used for palaeostress reconstruction (e.g.,  $n = 30$ ). Geology from Shobogorov (1977), Kuznetsov and Khrenov (1982) and Alexandrov (1989). (a) Palaeozoic stage 1, N–S compression in brittle–ductile conditions. Olkhon area, Central part of the Pri-Baikal belt. Structural pattern from Theunissen et al. (1993), T. Molchanova (pers. commun.), satellite image interpretation and field data. (b) Palaeozoic stage 2, NW–SE compression in the Pri-Baikal belt. Cross-sections redrawn from Melnikov et al. (1994). (c) Palaeozoic stage 3, E–W compression in the Pri-Baikal belt. (d) and (e) Mesozoic N–S compression in the South Baikal and Trans-Baikal area. Schematic cross-sections, vertical: not to scale.

(b)



(c)

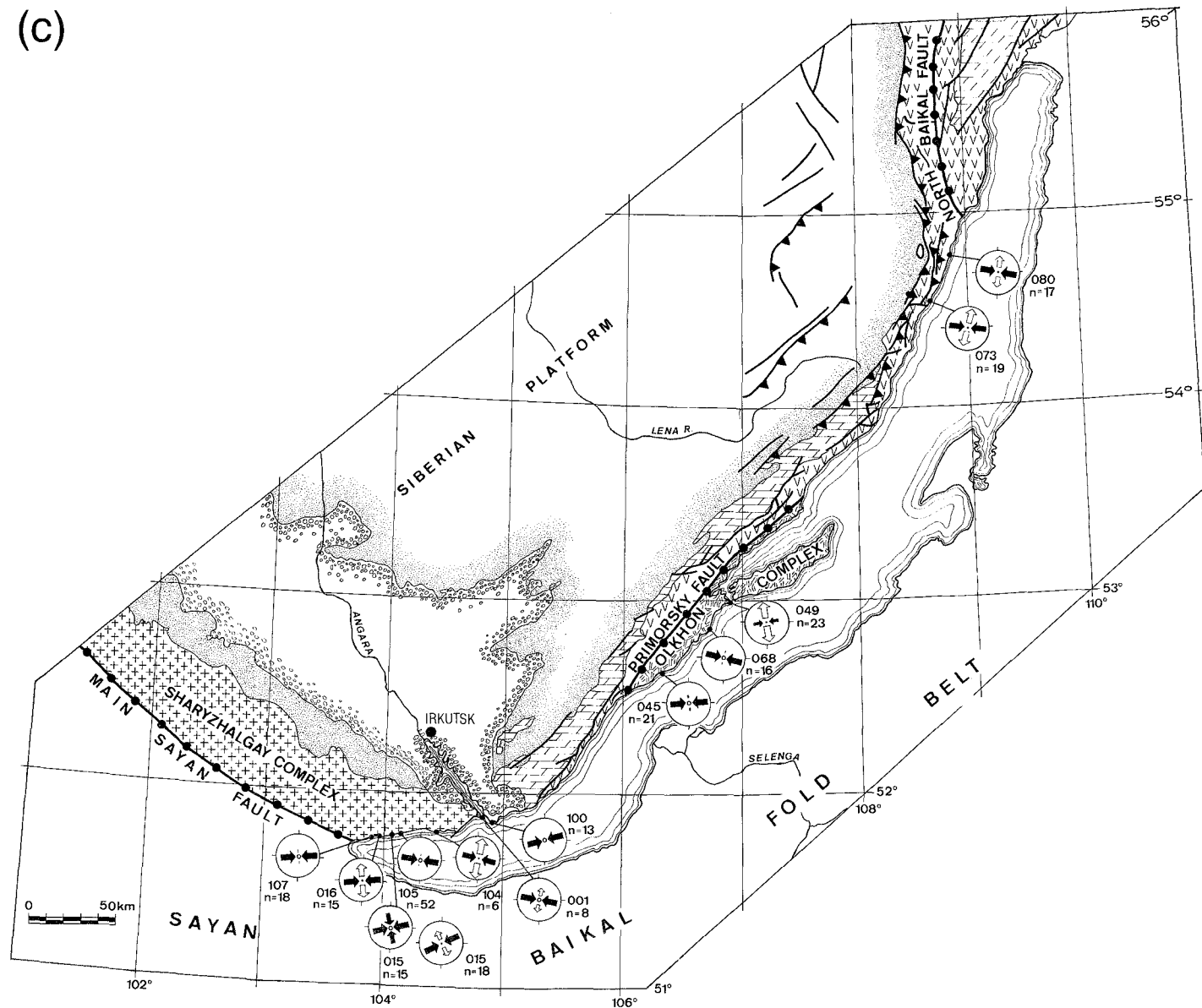


Fig. 4 (continued).

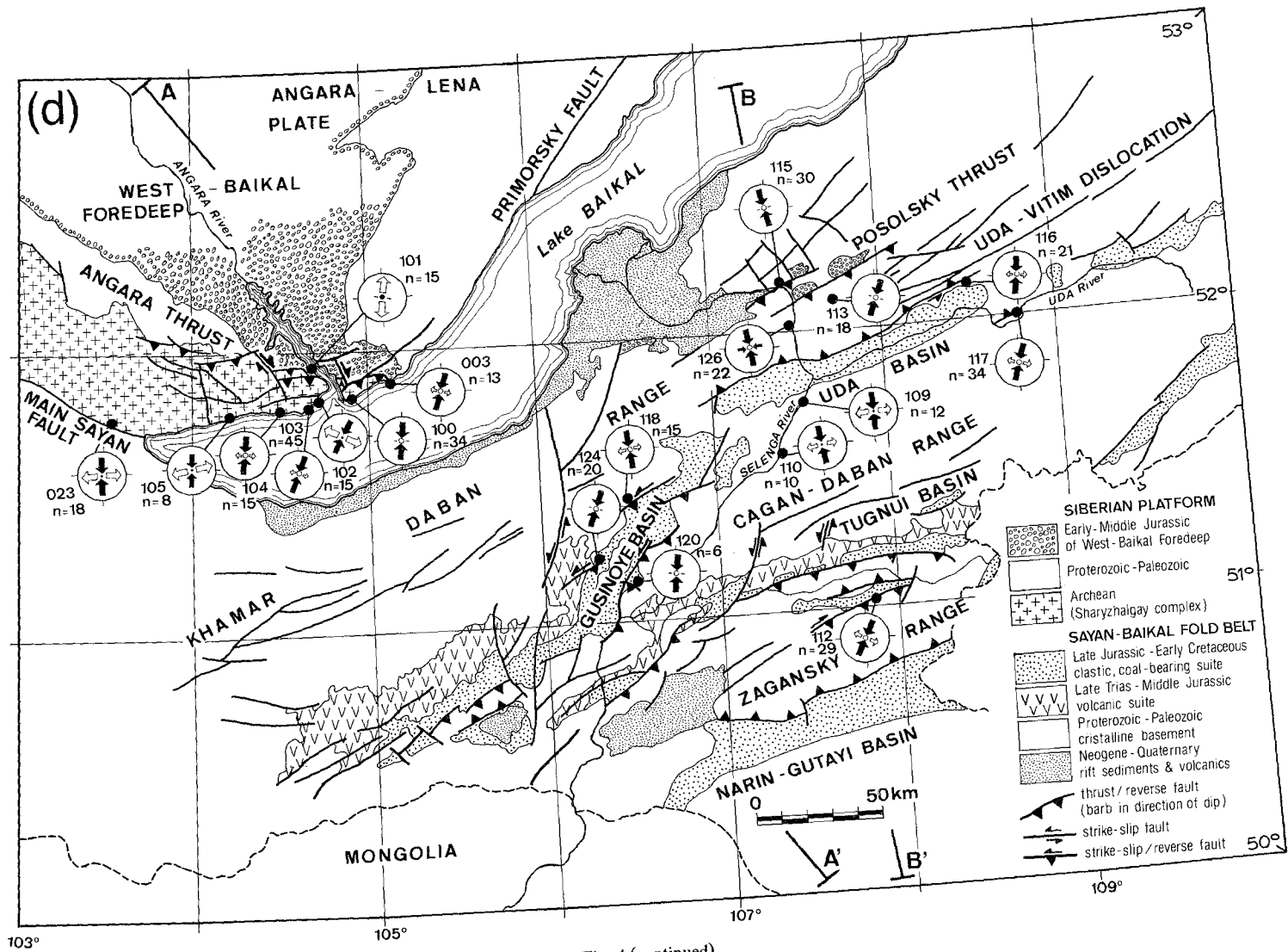


Fig. 4 (continued).

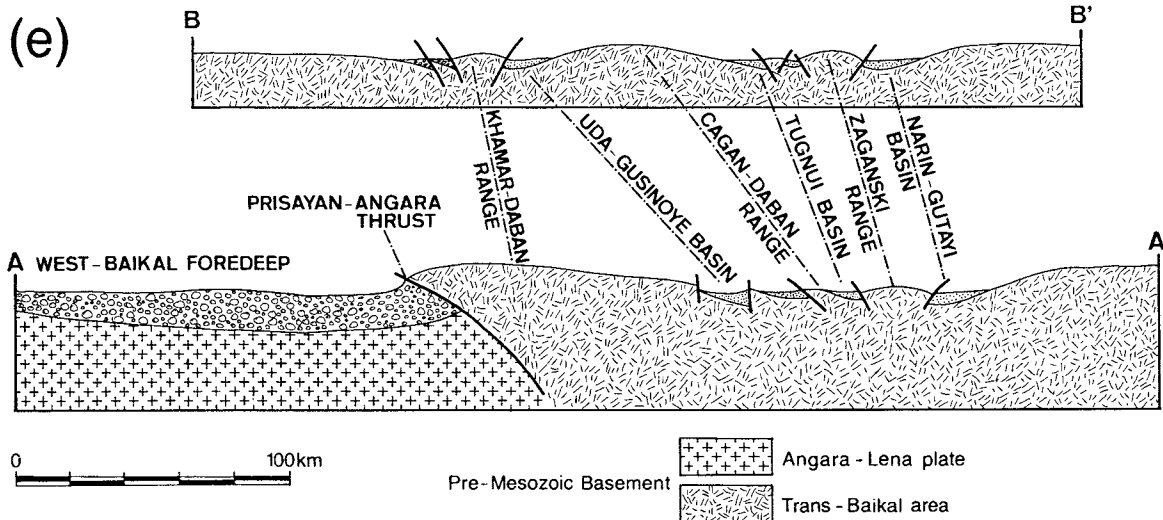


Fig. 4 (continued).

The second palaeostress regime has E–W (N101–281°E) horizontal principal compression and a sub-vertical intermediate axis (Fig. 4c). It caused mainly sinistral strike-slip movements along NW–SE faults that cut across the dominant NNE trend of the high-angle reverse faults (sites 80(2) and 73, Fig. 5).

### 3.3. Central Baikal: Primorsky dislocation and Olkhon complex

Along the western coast of Lake Baikal and in Olkhon Island, the tectonic suture between the Pre-cambrian basement at the margin of the Siberian platform and the Khamar Daban–Barguzin block is expressed by a major semi-ductile dislocation zone, known as the ‘Primorsky dislocation zone’ (Zamaraev et al., 1979; Theunissen et al., 1993). It separates the 1900 Ma old Primorsky rapakivi-type granite complex from the  $1890 \pm 25$  Ma high-grade gneisses of the Olkhon complex (U–Pb on zircons upper intercept, Bibikova et al., 1990). It affects both the Primorsky granite and the Olkhon gneisses by localized, but well developed belts of low greenschist facies mylonites to amphibolitic blastomylonites (Dobrzhinetskaya et al., 1992). Microstructural criteria (Theunissen et al., 1993) indicate that the dominant deformation mechanism is a sinistral lateral shear in a transpressive collisional context.

The Olkhon series are intruded by a belt of small mafic massifs (Ozorsky complex), including a large circular gabbro-norite intrusion (Birchim massif) with a Cambrian Sm–Nd age of emplacement (531 Ma; Bibikova et al., 1990). The Birchim intrusion has a massive core, but its external rim is variably affected by semi-ductile deformation at the contact with the surrounding shear zone (Fig. 4a). During the development of the shear zone, the Birchim massif obviously acted as a large-scale clast deflecting the trend of the semi-ductile flow during the sinistral transpressive deformation, indicating that the deformation is younger than the Birchim intrusion. A further age constraint is given by an Early Ordovician U–Pb lower intercept age on zircons for a gneiss of the Olkhon series, which dates the last strong metamorphic event ( $485 \pm 5$  Ma, Bibikova et al., 1990). Therefore, a Late Cambrian–Early Ordovician age can be proposed and this event can be related to the reactivation of the suture between the Khamar Daban–Barguzin block and the Siberian platform.

Microstructural investigations in the Olkhon area allowed to recognize both semi-ductile and purely brittle structures, from which palaeostress tensors were reconstructed (Table 1). They were attributed to three successive events, all of Palaeozoic age: Palaeozoic stages 1, 2 and 3 (Fig. 4a, 4b and 4c).

The first stage was recognized mainly in the

Pri-Olkhon region and corresponds to the semi-ductile deformation that affects the Primorsky granite and the Olkhon gneiss complexes along localized bands of intense shearing (Fig. 4a). Inside the mylonitic belts, microstructural textures are represented by mylonitic shear planes, often containing well developed tectonic lineation defined by stretched minerals. Southeast of the Birchim intrusion, the mylonitic foliation planes are steeply inclined, NE-trending and the tectonic lineations are also steeply inclined, with a mean azimuth direction to the

south-southwest (Fig. 6a-A). North of this intrusion, mylonitic foliation planes trend in a similar NE direction and are gentler inclined to the southeast ( $60\text{--}75^\circ$ ), with subhorizontal tectonic lineations (Fig. 6b-B). Palaeostress reconstructions were made by minimization of angular deviations between tectonic lineations and theoretical shear directions on foliation planes, assuming that mylonitic planes correspond to principal movement planes and that the tectonic lineations represent directions of maximum shear. The stress models show N–S horizontal direc-

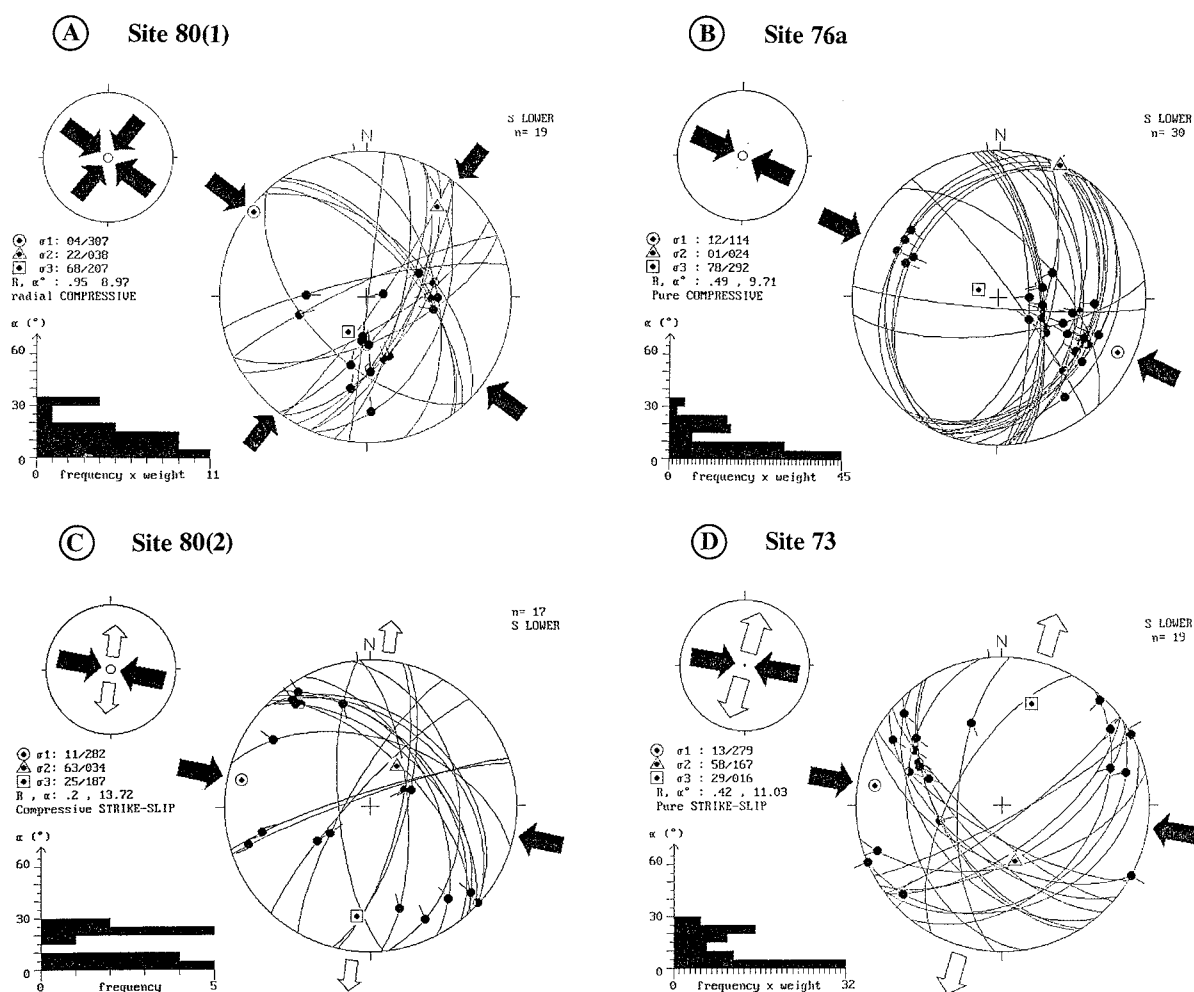


Fig. 5. Examples of palaeostress reconstructions for the North Baikal area. (A–B) Palaeozoic phase 2. (C–D) Palaeozoic phase 3. (A–C) Same site in Cape Cosa, with high-angle reverse faults affected by later strike-slip faults. (B) Low-angle thrust in Muzhinai cape. (D) Strike-slip faulting in Elochinn cape. Stereogram (Schmidt net, lower hemisphere) with traces of fault planes, observed slip lines and slip senses, histogram of observed slip-theoretical shear deviations for each fault plane and stress map symbols as in Fig. 3.

tions of compression for both areas, with a pure compressive regime for southwest Pri-Olkhon and a pure strike-slip regime for northeast Pri-Olkhon. This

corresponds well to what could be expected from the interaction of the Birchim massif with the surrounding structure in a transpressive context.

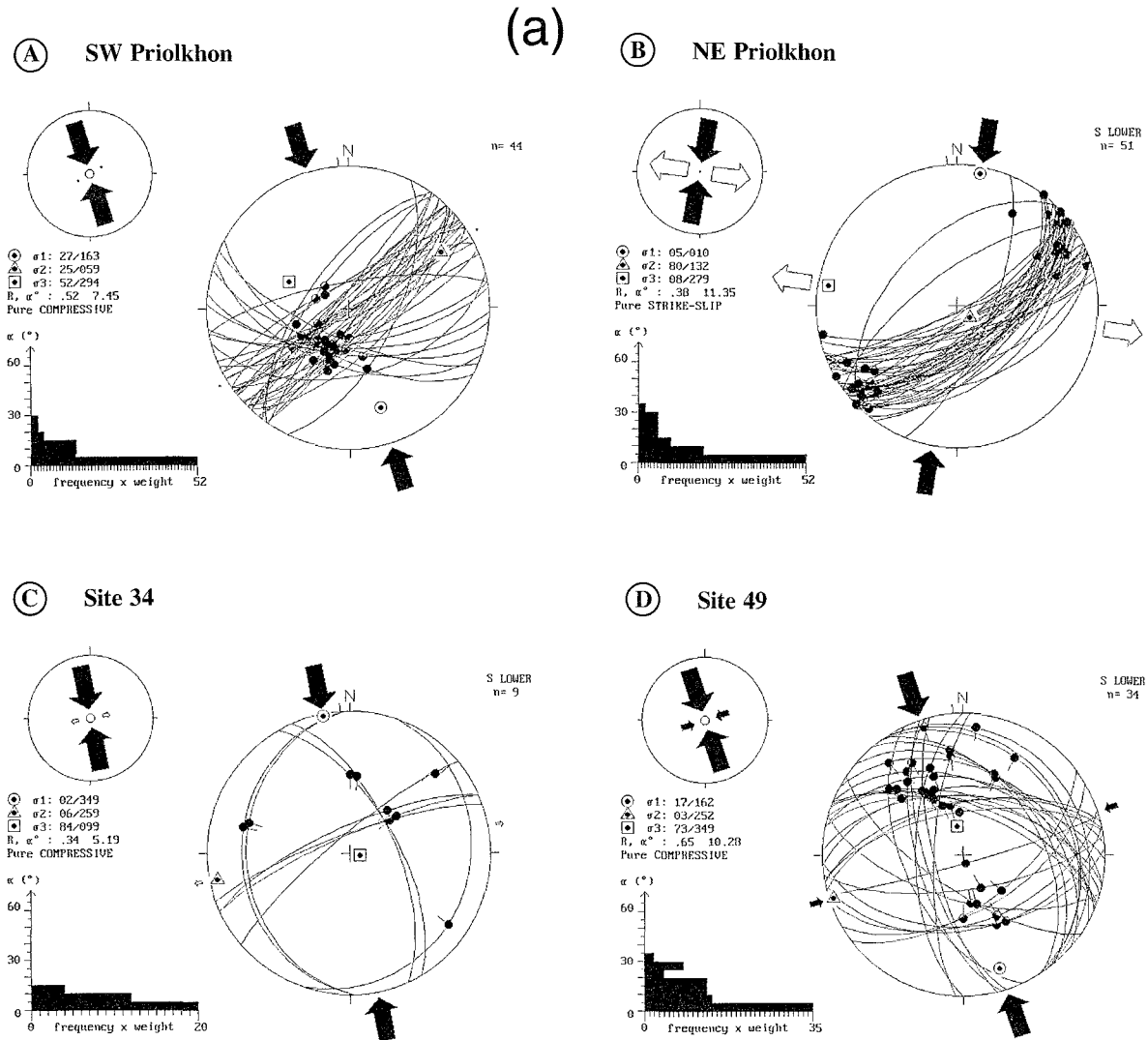


Fig. 6. (a) Examples of palaeostress reconstructions for the Pri-Olkhon region in Central Baikal. Palaeozoic stage 1, N–S compression. (A–B) Semi-ductile mylonitic planes with mineral extension lineation (used as movement planes and shear directions); stereograms and rose diagrams. (C–D) Brittle faulting in Primorsky granite (site 34) and Olkhon gneisses (site 49), not affected by the semi-ductile shear deformation (site 49). (b) Examples of palaeostress reconstructions for the Pri-Olkhon region in Central Baikal. (A–B) Palaeozoic stage 2 (NW–SE compression). (C–D) Palaeozoic stage 3 (E–W compression). (A) Strike-slip faults affecting the Primorsky sheared granite. (B) Thrust affecting Olkhon gneisses. (C) East-verging thrust system. (D) Strike-slip faulting in the Olkhon gneisses. (c) Comparative palaeostress reconstructions for the Pri-Olkhon region in Central Baikal. (A) Reverse faulting in unshered Primorsky granite (minimization of observed shear-theoretical slip deviations). (B) Fracture cleavage in Riphean dolomites, used as compression joints (maximization of normal stress magnitudes). (C) Shear cleavage and kink planes in Riphean shales, used as conjugated shear planes (maximization of shear stress magnitudes). Mohr diagrams with identical limiting friction lines (initial friction angles  $16.7^\circ$ , and ratio of extreme stress magnitude  $\phi = 0.25$ ).

Outside the mylonite belts, the original rapakivi texture of the Primorsky granite and the highly ductile texture of the high-grade Olkhon gneisses are relatively well preserved, and define undeformed lenses. Faulting is generally well expressed in them, and a system of palaeostress tensors with general N–S horizontal compression was clearly recognized (e.g., Fig. 6a-C, 6a-D). These N–S compressive tensors occur mainly in zones unaffected or weakly affected by the semi-ductile deformation. They were found over the whole Central Baikal area, along the Primorsky dislocation zone. The regional mean ten-

sor for brittle faulting is of a pure compressive type with a small component of strike-slip ( $R = 0.26$  Table 1), very similar to the tensors obtained for the semi-ductile deformation.

The reconstruction of palaeostress tensors from ductile structures is rather unusual and rely on the assumption that mylonitic planes correspond to principal movement planes and that tectonic lineation defined by stretched minerals represent directions of maximum shear. Because these assumptions could not be verified, only the palaeostress tensors reconstructed from brittle structures were used for calcula

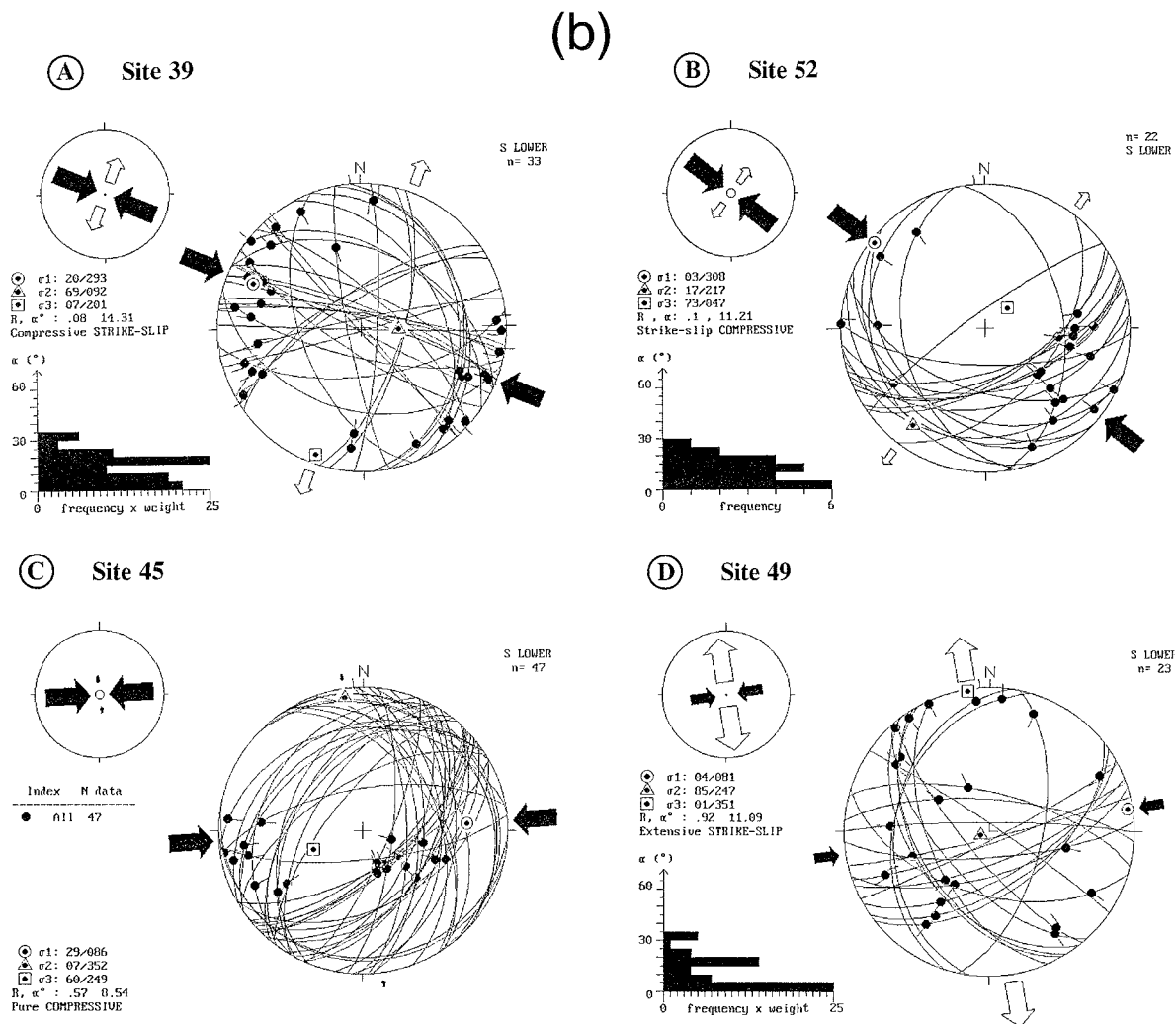
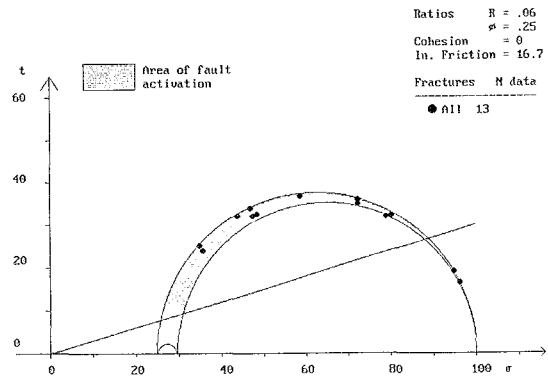
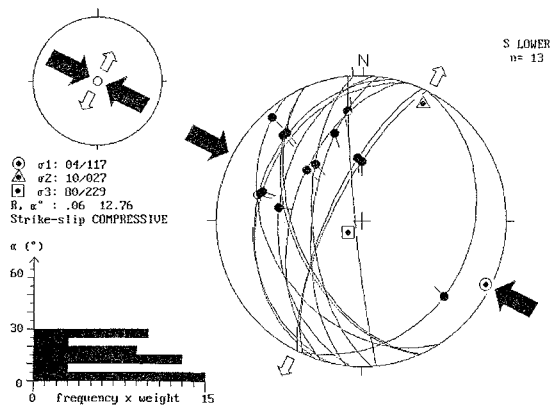


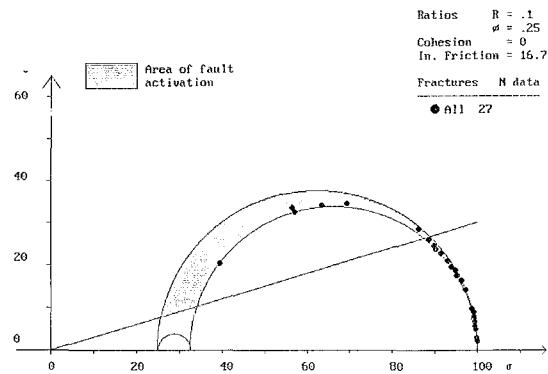
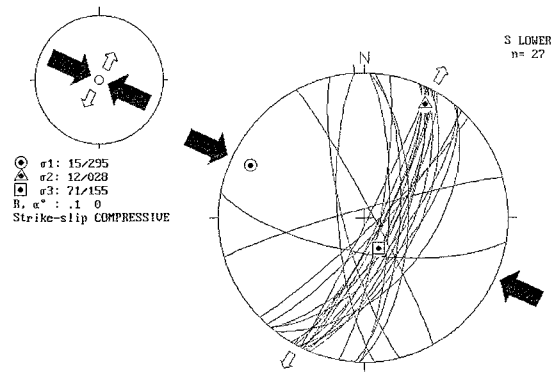
Fig. 6 (continued).

(C)

## (A) Site 36 (brittle faults in Primorsky granite)



## (B) Site 38 (fracture cleavage in Riphean dolomie)



## (C) Site 38 (shear cleavage and conjugated kink planes in shales)

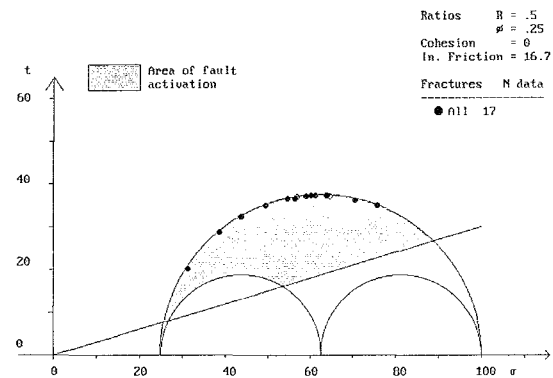
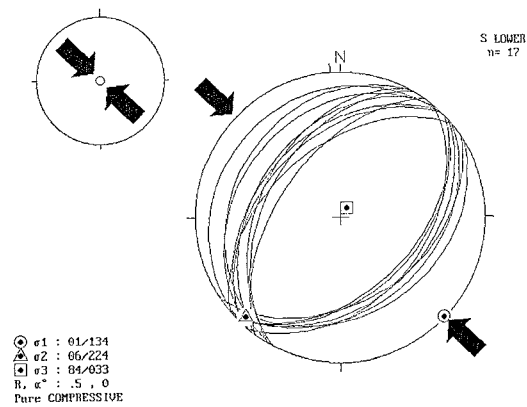


Fig. 6 (continued).

tion of the mean regional tensor. This deformation corresponds to the first brittle deformation recorded in the area (Palaeozoic stage 1).

Later stages of deformation are represented by purely brittle faults with cohesive cataclasites, that affect independently the mylonitic shear belts and the unshered lenses of the Primorsky granite and Olkhon gneiss. In the Riphean cover, which outcrops nearby in the Kurtun River, deformation is represented by folding and cleavage development. Tensors with NW–SE and E–W compression are respectively attributed to Palaeozoic stages 2 and 3 (Fig. 4b and 4c). In the Early Precambrian basement, they are represented by strike-slip and thrust or reverse faults (Fig. 6b). Some faults developed in the mylonitic texture of the Primorsky shear zone (site 39). In the Riphean cover, cleavage planes were also used for estimating the orientation of the three stress axes. In dolomites, fracture cleavage was considered as compression joints and stress axes were determined by maximization of normal stress magnitude on the planes (Fig. 6c-B). In slates, slaty cleavage was considered as shear planes, conjugated with well-developed kink planes, and stress axes were determined by maximization of shear stress magnitude on the planes (Fig. 6c-C). The resulting tensors are both of a compressive regime, with similar principal direction of compression. These are also fully compatible with a tensor computed for brittle faults in the underlying unshered rapakivi granite (Fig. 6c-A). This indicates that cleavage development in the Riphean corresponds to the same Palaeozoic stage 2, with general NW–SE horizontal principal compression.

#### 3.4. Southwest Baikal: Sharyzhalgay massif

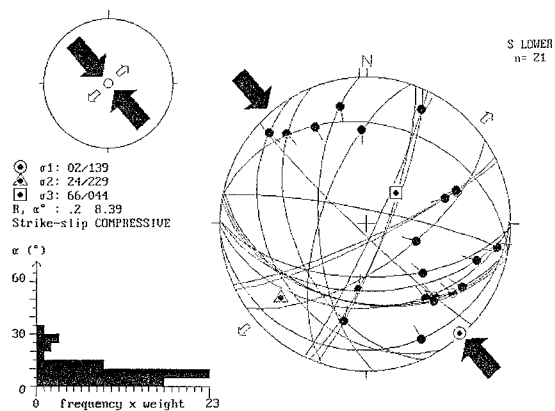
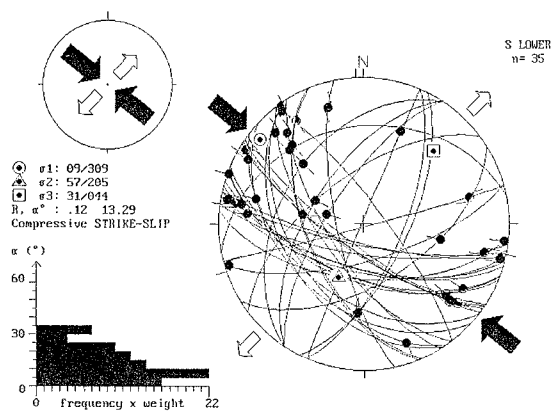
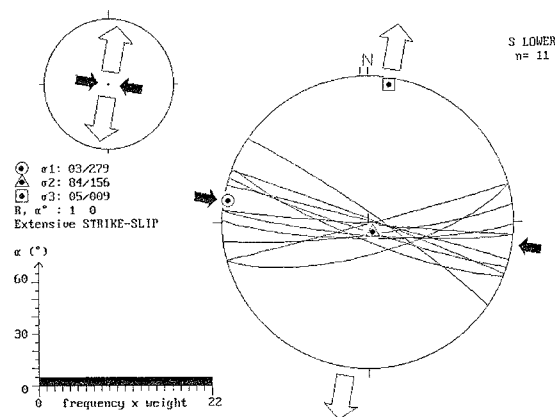
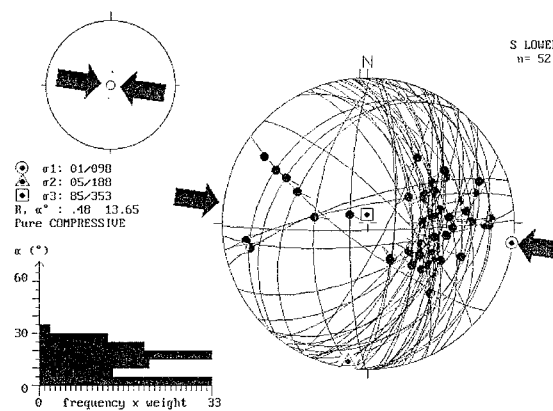
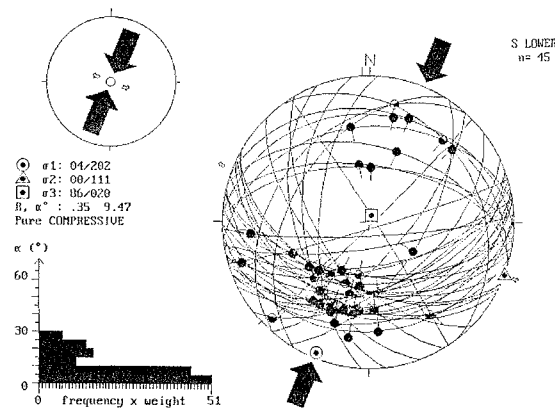
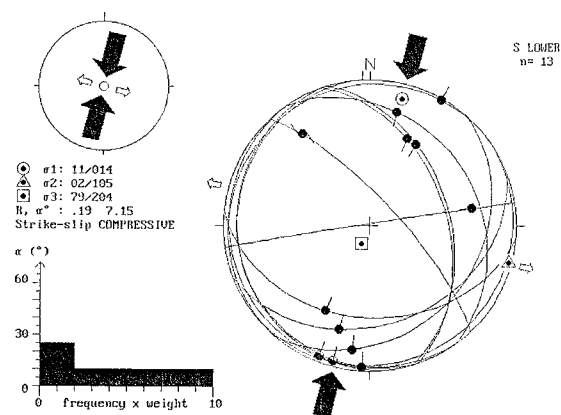
The Sharyzhalgay massif is composed exclusively of Early Precambrian rocks. It belongs to the Prisayan shield, a basement high at the margin of the Siberian platform. Despite its Early Precambrian age (Aftalion et al., 1991), a Cambrian imprint is indicated by 530 Ma basic dykes (Eskin et al., 1988), and by K/Ar reactivation ages of 565 Ma (hornblende), 515–500 Ma (phlogopite) and 480 Ma (biotite), reported by Manuilova and Koltsova (1969). Hercynian imprints are also indicated by a series of Carboniferous E-trending basic dykes dated at 332–296

Ma (Eskin et al., 1988) and by a 340 Ma K/Ar age on biotite (Manuilova and Koltsova, 1969). In the Mesozoic, this massif is involved in the north-vergent Prisayan–Angara thrust over the Jurassic platform cover (Fig. 4d).

In this Early Precambrian complex, direct age constraints for fault movement are only given by the presence of E-trending subvertical Carboniferous dykes. However, relative chronology can be indirectly established by estimates of relative depths of faulting, based on detailed observation of cataclastic textures. With depth, the fault texture changes from incoherent fault gouges to coherent cataclasites (with pseudotachylite, if dry), and to mylonites or semi-ductile deformation (Twiss and Moores, 1992).

The hard crystalline rocks of the Sharyzhalgay massif are intensely faulted. Large, generally multiphase, fault populations were measured from a nearly continuous section exposed along the old Trans-Siberian railway. The relative chronology is well constrained in site 103, by the presence of an E–W Carboniferous dyke (Fig. 7C). The tensor reconstructed by minimization of the normal stress magnitude on dyke planes indicates an E–W horizontal principal compression. Other sites with dominantly reverse faulting also refer to clear E–W compression (site 105 in Fig. 7D and site 107 in Fig. 8C). At site 103, the Carboniferous dyke crosscuts an earlier fault system, characterized by NW–SE horizontal compression (Fig. 7A, 7B) and sharp fractures without cataclastic texture. The dyke was also affected by a thrust system associated to incohesive cataclastite and earthy fault gouge (Fig. 8B). This later thrust corresponds to a N–S compression (Fig. 7E), of similar orientation as for site 003 on the Angara thrust fault itself (Fig. 7F).

According to our results, the Sharyzhalgay massif was affected by deformations due to three major compressive tectonic phases in the brittle domain. Referring to the regional palaeostress succession, the pre-dyke NW–SW compression can be attributed to the Palaeozoic stage 2 (Fig. 4b), the E–W compression contemporaneous to dyke injection to Palaeozoic stage 3 (Fig. 4c) and the N–W compression in superficial conditions to the Middle–Late Mesozoic stage (Fig. 4d). The Middle–Late Mesozoic stage and Palaeozoic stage 1 in the Olkhon area both show similar compressive type of tensor with N–S princi-

**(A) Site 103(1)****(B) Site 100****(C) Site 103(2): dykes****(D) Site 105****(E) Site 103(3)****(F) Site 003**

pal compression, but their very different depth conditions of evolution do not allow to associate them to the same event (respectively deep brittle conditions and shallow conditions with incohesive cataclastite and earthy fault gouge).

At site 107, an interesting case of faulting in brittle–ductile transitional conditions was recognized (Fig. 8C). A small fault displaces an amphibolite lens in a purely brittle manner, while at both extremities, the movement is entirely accommodated by ductile flow in the surrounding felsic matrix. The stress tensor obtained for a series of parallel faults indicates a typical E–W compression. This evidences very deep conditions of faulting in this block, during the E–W compressive event, in the brittle–ductile transition zone.

### 3.5. *Trans-Baikal: metamorphic core complexes and Mesozoic depressions*

The Trans-Baikal area corresponds to the Caledonian zone just southeast of the Siberian platform (Khangai–Yablonovy province of Ermikov, 1994). As reviewed above, the Trans-Baikal area is affected by the development of metamorphic core complexes in the Late Permian–Early Triassic and an en-echelon system of NE-trending alignments of volcano-sedimentary basins in the Mesozoic, separated by elongate narrow basement ridges.

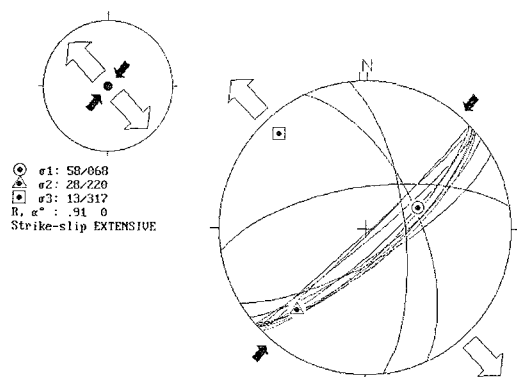
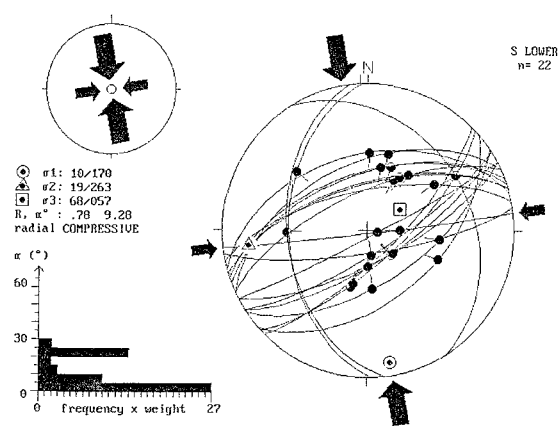
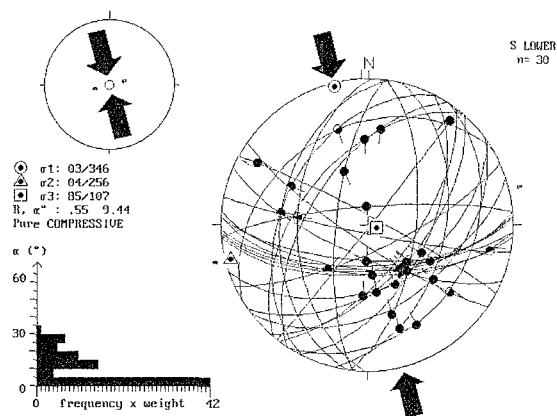
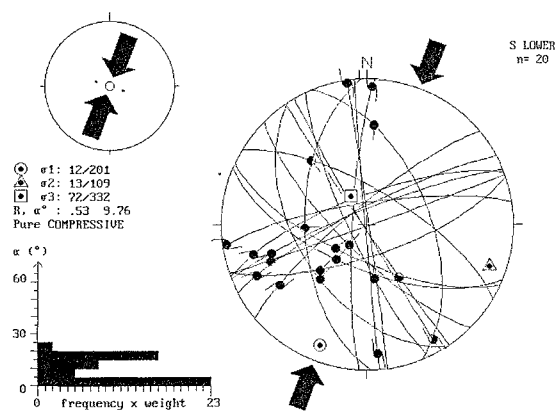
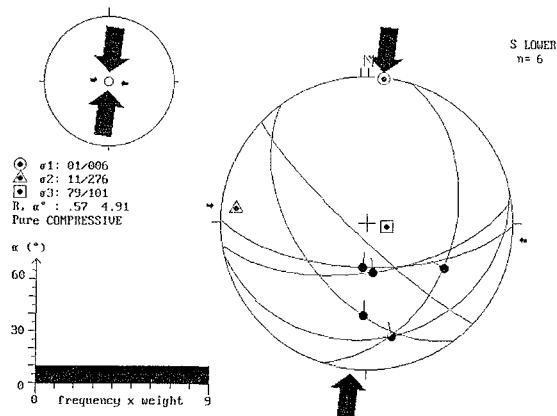
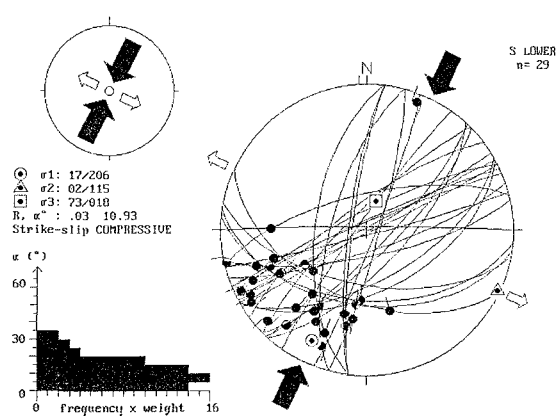
Adjacent to the Tugnui and Narin–Gutayi Mesozoic basins, the Zagansky block (Fig. 4d) was recently shown to be a Late Permian–Early Triassic granite–gneiss massif with much affinities to typical metamorphic core complexes of a Cordilleran type (Sklyarov et al., 1994). The Zagansky block is an antiformal structure, composed of granitic gneiss, with divergent low-dipping mylonitic foliation and unidirectional mineral lineation in a N150°E trend (Sklyarov et al., 1994). This NNW-trending mineral lineation is believed to indicate the direction of

principal extension during metamorphic core complex development. This direction is at a right angle to the strike of felsic dykes observed in the Khamar–Daban range (site 126), and for which a N140°E principal extension direction was obtained by using them as tension fractures in stress inversion (Fig. 9A). These dykes were reactivated later by reverse movements related to a N–S compression (Fig. 9B).

The structural map for the Mesozoic depressions (Fig. 4d) shows volcano-sedimentary basins, bounded by NE-trending faults and locally displaced by more latitudinal strike-slip faults. Microstructural measurements were collected in a large variety of settings, including intrabasinal crystalline basement blocks (site 126, Fig. 9B), major dislocation zones such as the Posolsky fault (site 115, Fig. 9C), the Uda–Vitim fault zone (site 116), along which developed the Uda and Gusinoye basins, and along the southern border fault of the Tugnui basin. Compressive to strike-slip tensors with mean N–S direction of principal compression were obtained for most of the measurement sites.

The relative age for this N–S compression is well constrained by structural and stratigraphic relations with Mesozoic volcano-sedimentary deposits. N–S compression was obtained for measurement sites in Cambrian (site 115), and Late Palaeozoic granites (sites 109, 110, 117 and 118), Early–Middle Jurassic andesite (site 124, Fig. 9D) and Early Cretaceous sediments (site 120, Fig. 9E). In addition, N–S compression was also obtained for sites in basement rocks, but along faults that affect the Mesozoic deposits or control the development of the basins. Site 112 (Fig. 9F) is located on the southern border fault of the Tugnui basin. This fault juxtaposes Early Cretaceous sediments with Late Permian–Early Triassic granite–gneiss of the Zagansky core complex and Carboniferous–Permian molasse. It has a dominantly strike-slip movement, with a slight reverse

Fig. 7. Examples of palaeostress reconstructions for the Early Precambrian Sharyzhalgay massif, South Baikal. (A–B) Palaeozoic phase 2, NW–SE compression. (C–D) Palaeozoic phase 3, E–W compression. (E–F) Mesozoic N–S compression. Site 103 indicates clear chronological relations, with (C) E–W basic dykes of Carboniferous age (Eskin et al., 1980) used as tension joints (minimization of normal stresses), (A) pre-dyke strike-slip faulting and (E) well-developed reverse faulting displacing the Carboniferous dykes (see also photograph in Fig. 8). Site 003 is on the Angara thrust fault, with both measurements in the Jurassic molasse and in the Precambrian.

**(A) Site 126(1): dykes****(B) Site 126(2)****(C) Site 115****(D) Site 124****(E) Site 120****(F) Site 112**

component. Sites 116, 118 and 124 are located along northern border faults of the Uda and Gusinoye basins.

In the volcano-sedimentary basins, no clear evidence was found for an initial stage of development in an extensive context. Instead, Ermikov (1994) reported several observations that sedimentation is related to reverse movements along the major border faults. He concluded that part of the Jurassic–Early Cretaceous development of the Trans-Baikal basins is related to a transpressional context. At the end of their evolution, from the end of Early Cretaceous to Late Cretaceous, younger thrust movements caused the partial closure of some basins, associated with trachybasalt eruptions and conglomerate formations. This is well expressed for the southern border fault of the Gusinoye basin, where a trachybasalt-injected fault caused the northwards thrusting of the Proterozoic basement over Early Cretaceous siltstone and lignite-bearing shales (site 120 in the Khoboldzhinsky quarry, Fig. 9E).

#### 4. Tectonic interpretation

In the basement of the Baikal rift zone, four major palaeostress regimes have been recognized. They are of a strike-slip to compressive type, with horizontal principal compression. They differ mainly by the orientation of their principal axis of compression ( $\sigma_1$ ), by the areal distribution of their manifestations and by the type of associated cataclastic textures. In addition, there are also indications for a Late Palaeozoic–Early Mesozoic extensional stage, but this one is not actually documented by brittle microstructures. According to structural and stratigraphical relationships, the palaeostress stages have been successively classified as follows: (1) N–S compression, in brittle–ductile conditions (Early Palaeozoic); (2) NW–SE compression (Middle Palaeozoic); (3) E–W com-

pression (Late Palaeozoic); (4) NNW–SSE extension (Late Palaeozoic–Early Mesozoic); and (5) N–S compression, in relatively superficial conditions (Middle–Late Mesozoic).

The effects of the three compressive Palaeozoic stages were observed along the whole length of the western coast, exclusively in Precambrian rocks. Therefore, a direct age estimate from stratigraphic relations is impossible, but they can be related to known tectonic events evidenced from basic geological work, and confirmed recently by modern geochronological data. For the Mesozoic stage, the age is better constrained by stratigraphic and structural relations. A regional synthesis of palaeostress evolution for the Baikal pre-rift basement is presented in Fig. 10, based on computation of mean stress tensors for subregional divisions.

As already discussed, the *Early Palaeozoic stage 1* corresponds to semi-ductile sinistral transpressive movements along the Primorsky shear zone, and to purely brittle faulting in the remaining massifs preserved from the shear deformation. The timing of this event is indirectly constrained by the Late Cambrian–Early Ordovician age for the metamorphism associated to semi-ductile deformation. The Primorsky shear zone belongs to the marginal suture between the Siberian platform and the Sayan–Baikal fold belt. It lies in the eastern prolongation of the Main Sayan shear zone which borders the Sharyzhalgay massif. Northeastwards, an underwater extension of the Primorsky shear zone is postulated by Bukharov et al. (1993), from deep-water observations with the *Pisces* submarine. No clear expression of a possible continuation of the Primorsky shear zone was noticed on the eastern coast of Lake Baikal (Barguzin block). However, the basement of the Barguzin block is largely hidden by widespread granitization in Palaeozoic times. It is therefore not clear whether (1) the NE-trending Primorsky shear zone is progressively bent in a more N–S trend and

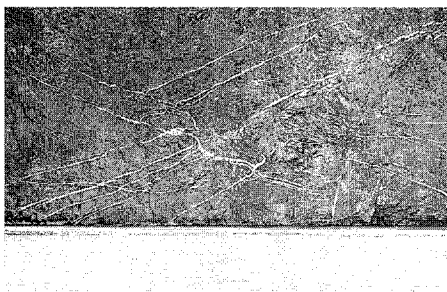
Fig. 8. Outcrop photographs. (A) Thrust system contemporaneous to a felsic dykes injection in the Pri-Olkhon massif, along the lake shore (B) E-trending Permian basic dyke in the Sharyzhalgay massif, affected northwards thrusting with unconsolidated cataclastic fault gouge (site 103, outcrop height is 6 m). (C) Brittle–ductile fault in the Sharyzhalgay massif (site 107), displacing an amphibolitic lens in a brittle manner and accommodated by ductile flow in the surrounding felsic matrix: (C1) general view (scale given by pen); (C2) related stereogram and palaeostress determination; (C3, C4) details of western and eastern terminations of the fault.

links with the North Baikal fault zone, or (2) it originally continued in the Barguzin block, or (3) it progressively disappears northeastwards.

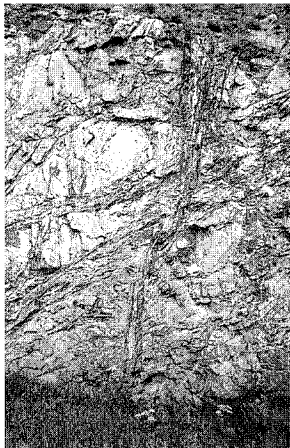
The *Middle Palaeozoic stage 2* (NW–SE compression) is associated to the thrust and reverse fault structure that characterizes the Pri-Baikal fold-and-thrust belt. A Late Silurian–Early Devonian age of

this tectonic event is indirectly constrained by the stratigraphic gap in the sedimentary cover of the Siberian platform, by K–Ar reactivation ages along the Pri-Baikal belt (Manuilova and Koltsova, 1969), and by the unconformable position of Middle Devonian continental molasse. In North Baikal, the subregional stress field is compressive to constrictive

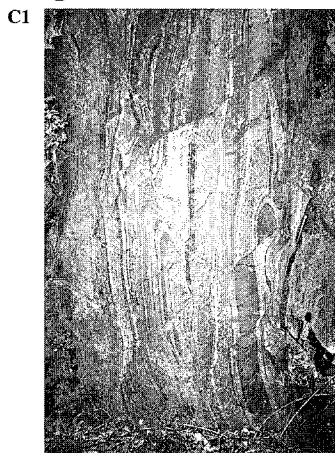
Ⓐ Priolkhon massif



Ⓑ Site 103

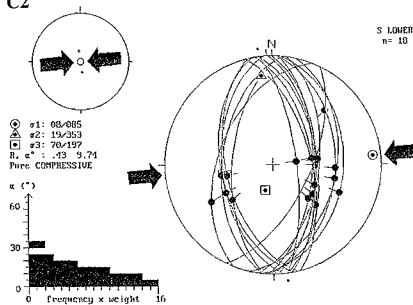


Ⓒ Site 107

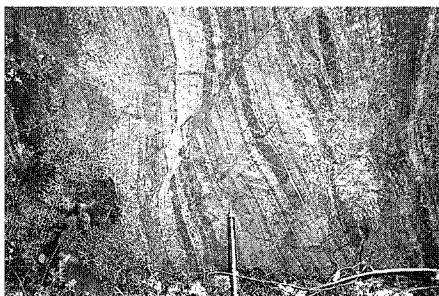


W <----- 140 cm -----> E

C2



C3



C4



| Stages<br>Age                            | Paleozoic 1<br>L. Cambr. - E. Ordov. | Paleozoic 2<br>M. + L. Silurian | Paleozoic 3<br>Carboniferous | Mesozoic<br>M. Jurass - E. Cret. |
|--|--------------------------------------|---------------------------------|------------------------------|----------------------------------|
| North-<br>Baikal                         |                                      |                                 |                              |                                  |
| Central-<br>Baikal<br>(Oikhon)           |                                      |                                 |                              |                                  |
| South -<br>Baikal<br>(Shary-<br>zhalgay) |                                      |                                 |                              |                                  |
| Trans -<br>Baikal<br>(Posolsky)          |                                      |                                 |                              |                                  |
| Trans -<br>Baikal<br>(Uda -<br>Gusinoye) |                                      |                                 |                              |                                  |

Fig. 10. Synthetic table of regional stress tensors for Palaeozoic and Mesozoic compressive stages in the Baikal region.

(vertical  $\sigma_3$  and  $R = 0.75$ ), and related to extensive development of thrust sheets and reverse faults along the Baikal coast, together with the development of a large-scale detachment in the Middle Riphean level of the platform cover (Fig. 4b, section A–A'). In both Central and South Baikal, the stress regime is transitional between compressive and strike-slip. It is associated to intense strike-slip and reverse faulting

in the Precambrian basement and folding with cleavage formation in the Riphean cover. In Central Baikal, the Primorsky semi-ductile shear zone was not reactivated during this second event. Instead, it was dissected by numerous subvertical strike-slip faults, at a high angle to the shear zone.

The major consequence of this tectonic stage on the pre-rift structural fabric, was the development of

Fig. 9. Examples of palaeostress reconstructions for the Trans-Baikal area. Mesozoic N–S compression. (A) Felsic dykes of site 126 in the Khmar Daban block, used as tension joints (minimization of normal stresses). (B) Post-dykes faulting in the same site 126, partly reactivating the dyke surfaces. (C) Reverse faulting along the Posolsky thrust. (D) Strike-slip faulting in Early–Middle Jurassic andesite lavas along the northern border of Gusinoye depression (Uda–Vitim dislocation). (E) Thrust fault injected by trachybasalt, affecting Early Cretaceous siltstones and shales at the southern border of the Gusinoye depression. (F) Southern border fault of the Tugnui basin separating Early Cretaceous from Precambrian granite (later reactivated in Cenozoic).

low-angle thrusts and high-angle reverse faults along most of the western coast of Lake Baikal, which were preferred sites of reactivation during the Cenozoic. This strongly influenced the development of the Baikal depression during rifting, as shown by the good accordance between the major border faults of the Baikal depression and the general trend of the Pri-Baikal belt.

The *Late Palaeozoic stage 3* (strike-slip stress regime, E–W compression) is characterized by a regional evolution of palaeostress tensors, with progressive increase in the relative magnitude of the maximum principal stress axis ( $\sigma_1$ ), from NW to SE. In North Baikal, the stress regime is pure strike-slip ( $\sigma_2$  vertical,  $R = 0.31$ ). In Central Baikal, it evolves into compressive strike-slip ( $\sigma_2$  vertical,  $R = 0.01$ ). In South Baikal, it is strike-slip compressive ( $\sigma_3$  vertical,  $R = 0.22$ ). For the Late Palaeozoic stage, the age constraints are poor. The age is bracketed in the Devonian–Early Permian period, between the Late Silurian–Early Devonian event in the Pri-Baikal belt and the Late Palaeozoic–Early Mesozoic development of metamorphic core complexes in Trans-Baikal. In the absence of more precise indications, it is tentatively postulated that the E–W compressive stress regime may have been contemporaneous to the development of E–W Carboniferous basic dykes in the Sharyzhgaly massif.

The *Late Palaeozoic–Early Mesozoic stage 4* (NNW–SSE extension) is marked by a period of intense crustal extension in the Trans-Baikal area, with the development of metamorphic core complexes, dyke emplacement and voluminous magmatism. The extension direction is inferred from the mineral lineation in the mylonitic foliation of the Zagansky metamorphic core complex, and by the ENE-trending dykes in the Khamar Daban block, along the Selenga River. In the superficial units, above the Zagansky core complex, extensional faulting is not actually documented by field observations, but our investigation in this area was too preliminary to conclude in the absence of expression of extensional faulting.

The *Middle–Late Mesozoic stage 5* (N–S compression) affects differently the southern margin of the Angara–Lena plate and the Trans-Baikal region. For this stage, the stratigraphic control is very clear, and a Middle Jurassic–Early Cretaceous age can be

proposed. The presence of strike-slip faults cutting obliquely the mylonitic fabric of the Zagansky granite–gneiss and the strike-slip reactivation of the felsic dykes of the Khamar Daban range indicate clearly the relative succession from extensional to compressional stages in the Mesozoic Trans-Baikal. The development of Mesozoic sedimentary basins in South-Siberia and Mongolia started in the Early Jurassic, after a general unconformity in the Middle Triassic and a volcanic phase in the Late Triassic (Ermikov, 1994).

On the southwestern margin of the Angara–Lena plate, the Early–Middle Jurassic West-Baikal foredeep developed. It is actually limited to the south by the Prisayan–Angara south-dipping thrust. Southwards coarsening and facies evolution of the sediments indicate that sedimentation in the West-Baikal foredeep was controlled by the development of the Prisayan–Angara fault. Later movements caused the partial thrusting of the Early Precambrian Sharyzhgaly massif over the Jurassic platform cover. In a large-scale N–S cross-section (Fig. 4d, section A–A'), the present structure is typical of a compressive half-ramp basin, but it is not precisely known whether it evolved initially as an extensional basin, or if it remained for the whole Jurassic period in a compressive setting. Cobbold et al. (1993) illustrates examples of Cenozoic sedimentary basins developed by crustal thickening in Central Asia (Junggar, Tarim, Issyk-Kul and Fergana basins), and compared them to experimental models. The present West-Baikal foredeep can also be considered as an example of half-ramp basin development on the margin of the Siberian platform, at least for its final stage. Northwards, a long-wavelength buckling of the lithosphere caused successively a basement flexural uplift in the Bratsk area, and a linear depression filled by Jurassic sediments in the central part of the Siberian platform (Figs. 1 and 11F). The total wavelength of the lithospheric buckle reached 700 km, from the Prisayan–Angara thrust to the centre of the Siberian platform.

In the Trans-Baikal area, a series of 10–15-km-wide, 100–120-km-long basins developed along echelon zones, separated by 50–60-km-wide basement horsts. Their structural pattern was controlled by reactivated basement faults inherited from the Late Palaeozoic period. These basins are generally

regarded as resulting from Mesozoic extension (Trans-Baikal rift system of Lobkovsky et al., submitted), but the recent compilation of Ermikov (1994) and our present structural investigation indicate that a significant part of the history of their development occurred in a compressive context, probably in the Early–Middle Cretaceous. During the Late Jurassic–Early Cretaceous, they developed with a progressive inversion from extensional to compressional tectonics. In the final stage, intense compressive tectonics is clearly manifested from the end of the Early Cretaceous to the beginning of the Late Cretaceous. This later event caused thrusting of the crystalline basement over Jurassic–Cretaceous sediments, e.g., along the southern borders of the West-Baikal foredeep and the Gusinoye basin.

The border faults of the Uda–Gusinoye, Tugnui and Narin–Gutayi basins have reversed to strike-slip movements. This structural pattern is again typical of ramp-style sedimentary basins. A N–S cross-section in the Trans-Baikal area displays the typical structure of full-ramp and half-ramp basins of different polarity, separated by basement blocks (Fig. 4D, sections A–A' and B–B').

Results of a last field expedition, conducted after the submission of this article, confirmed the existence of large-scale oblique reverse to left-lateral movements along northeast-trending faults in the Palaeozoic Angara–Vitim granitoids of the Barguzin block, associated with a dominantly N–S direction of maximum compressive stress.

The Late Triassic volcanism and the initial development of the Mesozoic depressions in the Early–Middle Jurassic can be related to the latest stages of the extension in a thinned and hot lithosphere. After tectonic inversion, in the Late Jurassic–Early Cretaceous, the Middle–Late Cretaceous sedimentation occurred in a compressive to transpressive context. This marks the final evolution of the Mesozoic basins, before a long period of stability and penplanation in the Late Cretaceous–Paleocene.

## 5. Geodynamic implications

Recent investigations of the intraplate stress field (Zoback et al., 1989) evidence three important observations, that allow Richardson (1992) to postulate

that the intraplate stress field should contain information on the driving mechanism for plate tectonics. The first general observation is that the dominant intraplate stress in the present world situation is compressional. Extensional intraplate stresses occur mainly in regions of elevated topography and are not necessarily of a plate tectonic origin. Secondly, the world-wide stress compilation of the ILP World Stress Map Project (Zoback, 1992) shows the existence of large regions of uniform stress orientations, reflecting a large-scale tectonic process. A strong correlation between directions of maximum horizontal stress and absolute plate motion was demonstrated for several large regions of uniform stress field, such as North America and Western Europe (Richardson, 1992).

Amongst the forces postulated as generating the intraplate stress field and governing the plate driving mechanism, ridge push forces arising from the time-dependent cooling and thickening of oceanic lithosphere is generally considered to be the dominant one (Richardson, 1992). Collisional resistance forces in continental collisions may also play an important role, as in the present collision of India with Eurasia (Cloetingh and Wortel, 1986). In subduction zones, the two major forces are negative buoyancy of the slab and resistance of the slab entering the mantle. These forces act in opposite sense and the resulting force is small (Forsyth and Uyeda, 1975). Other forces may also be linked to petrological transformations, such as eclogitization processes.

The origin of the horizontal compressive palaeostress field that was evidenced for the Sayan–Baikal fold belt in the Palaeozoic and Mesozoic periods should be examined in the light of the above features of the global intraplate stress field. In the case of Central Asia, the regional importance of the reconstructed palaeostress fields is indicated by the homogeneity of the palaeostress tensors and the consistency of orientation of the horizontal principal stress axes over a large area (650 km between both ends of Lake Baikal). It can therefore be postulated that the regional stress fields correspond to the dominant kinematic events of plate tectonic origin.

The following palaeogeodynamic reconstructions are adapted from Enkin et al. (1992), Sengör et al. (1993), Zorin et al. (1993), Berzin et al. (1994) and Belichenko et al. (1994), in function of the regional

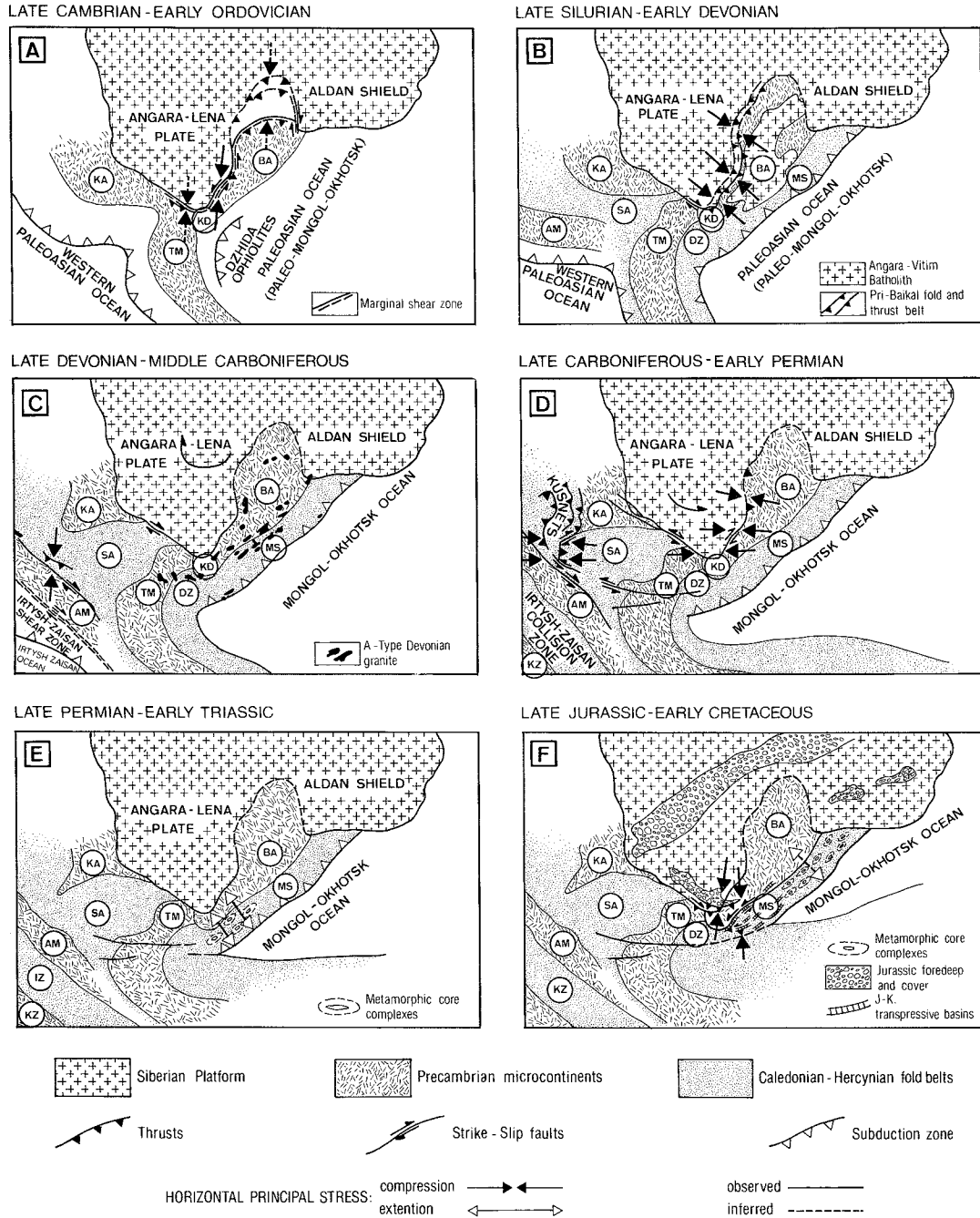


Fig. 11. Palaeogeodynamic sketches for the Palaeozoic and Mesozoic palaeostress stages in the Baikal area, Central Asia. Adapted from Sengör et al. (1993), Zorin et al. (1993), Berzin et al. (1994) and Belichenko et al. (1994). All sketches are presented in present-day coordinates. Precambrian microcontinents: *TM* = Tuva–Mongolia, *KA* = Kansk–Derba, *AM* = Altai–Mongol, *KD* = Khamar Daban, *BA* = Barguzin, *KZ* = Kazakhstan. Caledonian–Hercynian terranes: *DZ* = Dzhiba, *MS* = Mongol–Stanovoy, *SA* = Sayan, *IZ* = Irtysh–Zaisan.

directions of horizontal stress axes obtained for the successive palaeostress stages. They are discussed with reference to present-day coordinates. These are different from absolute coordinates, due to important rotation and translation movements involved in the plate kinematics. The accretion of terranes to the Siberian platform, progressively increased the area of the 'stable' Siberian plate. It can be assumed that once a new block has been incorporated to the Siberian continental mass, it did not suffer important subsequent movements relatively to the Siberian craton itself. This may apply particularly for the region of the Baikal rift zone, while for the Altai region it is more speculative. Therefore, the following discussion should be understood with reference to a relative fixed position of the Siberian platform. For the absolute coordinates and description of the rotation of lithospheric plates, the reader should refer to Sengör et al. (1993) and Berzin et al. (1994).

### 5.1. *Early Caledonian lateral reactivation*

After the initial accretion of the Khamar Daban–Barguzin microcontinent to the Siberian platform in the Vendian–Cambrian, renewed interaction between the Khamar Daban–Barguzin microcontinent and the Siberian platform is responsible for the Late Cambrian–Early Ordovician semi-ductile transpressive deformation observed along the Primorsky dislocation zone. This shear zone is considered as part of the marginal suture of the Siberian platform (Melnikov et al., 1994). The dominant movement indicated by narrow zones of high semi-ductile deformation is sinistral strike-slip, with a slight reverse component. The mean stress tensor, reconstructed for brittle faults from sites preserved from the deformation, indicates a pure compressive regime, with a N–S principal direction of compression. These data are compatible with the mechanism of northeastwards translation of the Khamar Daban–Barguzin block along the southeastern margin of the Siberian platform, similar to lateral accretion (Fig. 11A). No detailed structural data are available for other segments of the suture zone between the Khamar Daban–Barguzin block and the Siberian platform, but a similar N–S compression can be inferred for the surrounding areas. In the Vitim embayment, a frontal collision is inferred from the presence of large-scale north-verging

thrusts, and the corresponding interruption of Vendian–Early Cambrian sedimentation on the Barguzin block and in the Mama–Bodajbo foredeep. The suture zone may correspond to the North Baikal ophiolite zone (Dobretsov et al., 1992; Konnikov et al., 1993) but more detailed geochronological work is necessary to draw final conclusions. Along the southern edge of the Angara–Lena plate, a geophysical investigation confirmed that the Tuva–Mongolia microcontinent collided with the Siberian platform, along a south-dipping subduction zone (Zorin et al., 1993).

This early Caledonian collision closed the Palaeo-Asian ocean along the southern margin of the Siberian platform, causing accretion of microcontinents south of it. The subduction zone shifted southwards, to the Dzhida ophiolite zone, possibly also south-dipping. Individualisation of a new oceanic area, south and east of this enlarged continental zone, marks the beginning of the history of the Palaeo-Mongol–Okhotsk branch of the Palaeo-Asian ocean.

### 5.2. *Late Caledonian frontal collision*

The Late Silurian–Early Devonian folding and thrusting in the Pri-Baikal belt affected the southeastern margin of the Angara–Lena plate along its contact with the Khamar Daban–Barguzin block, as the response to regional NW–SE horizontal compression. At that time, the Khamar Daban–Barguzin block was already attached to the Siberian platform, as shown by the geology of the Olkhon area in Central Baikal. A subduction zone was active along the southeastern margin of the Khamar Daban–Barguzin block during the Ordovician and Silurian. The Dzhida ophiolite zone belonged to an island-arc system in front of a south-dipping (?) subduction zone, active in the Late Ordovician–Silurian. The regional NW–SE horizontal principal compressor recorded in the Pri-Baikal belt is consistent with a frontal collision of this island-arc system with the Tuva–Mongolia and Khamar Daban–Barguzin continental chain. The accretion probably took place along the Uda–Vitim zone and enlarged the Palaeozoic continental mass surrounding the southern margin of the Siberian craton by incorporation of a new Caledonian rim (Dzhida ophiolites and Mongol–Stanovoy

zone). The Late Caledonian suture zone may correspond to the Uda–Vitim zone (also known as Selenga–Vitim zone). This zone is poorly defined in the surface geology, but has a more clear geophysical expression. Ophiolites are known along its northern segment (Gibsher et al., 1993).

A new subduction zone developed with reversal polarity at the back of the newly accreted terranes, probably contemporaneously to the collisional stage. This caused large-scale S-type granitic magmatism in the Dzhida, Khamar Daban–Barguzin and Mongol–Stanovoy terranes (Trans-Baikal area), obliterating most of the earlier structures (Fig. 11B). It marks the beginning of the Mongol–Okhotsk ocean *sensu stricto*.

In this model, the Pri-Baikal belt may have arisen from accretion of new continental masses to the back side of the Khamar Daban–Barguzin block, along the Uda–Vitim zone. Despite the granitic invasion, this block was rigid enough to transmit the stress field to the suture zone with the Siberian platform, which was intensely reactivated (Pri-Baikal fold-and-thrust belt).

### 5.3. Hercynian strike-slip reactivation

During the Devonian, the Tuva–Mongolia continent began to bend progressively in a counter-clockwise manner, while the oceanic lithosphere of the Mongol–Okhotsk ocean subducted to the north, under the Khamar Daban–Barguzin block, at the southern margin of the Siberian plate. The Trans-Baikal area then was in a situation of Andean-type active margin, and was affected by numerous small granitic intrusions. To the west, an oblique subduction zone was active in the Devonian, along the southwestern margin of the Altai–Mongol block. Progressive closure of the Irtysh–Zaisan branch of the Palaeo-Asian ocean led to the collision of Kazakhstan with Sayan and Tuva–Mongolia in the Altai area during the Early Carboniferous. Intense right-lateral shearing occurred along the Irtysh–Zaisan blastomylonite belt.

The geodynamic interpretation of palaeostress 3 is relatively speculative, due to poor age constraints. As suggested in the tectonic interpretation, the source of this stress field is probably related to the closure of the Irtysh–Zaisan ocean in the western part of Central Asia. The reconstruction for this stage includes unpublished preliminary results from a struc-

tural and palaeostress investigation in the Altai area, in the summer of 1993, with N. Berzin. This investigation indicates the existence of two successive compressive stress fields in the Altai massif, with respective N–S and E–W directions of principal compression. The first stage affected Vendian to Middle Devonian granites and clastic sediments, and the second acted upon these rocks together with Late Carboniferous–Early Permian granites and limnic deposits. The first stage of compression is therefore constrained to the Late Devonian–Middle Carboniferous period. It has no equivalent in the Baikal region. The second stage is correlatable with the third compressional stage in the Baikal region, due to their common E–W principal direction of compression. In the Baikal region, the timing of this third stage is only constrained by its possible association with E–W-trending Carboniferous dykes in the Sharyzhalgay massif.

Keeping in mind that one of the major sources of intraplate compressive stress field is collisional tectonics at plate boundaries, the N–S compression observed in Altai can be related to the collision of Kazakhstan with the Sayan and Tuva–Mongol blocks in the Early Carboniferous (Fig. 11C). The geographical location of the collision zone and the N–S polarity of the stress field explain why this stress field was not recorded in the Baikal area. However, it may have influenced the Palaeozoic basement of the West Siberian basin.

In absence of better age constraints, the E–W compression observed in both Altai and Baikal regions is tentatively related to the latest collisional stage evidenced by Allen et al. (1992), which marks the final closure of the Irtysh branch of the Palaeo-Asian ocean in the Late Carboniferous–Early Permian (Fig. 11D).

In the absolute coordinates, palaeomagnetic data indicate that the whole Siberian continental mass rotated clockwise from the Silurian to Carboniferous and counter-clockwise from the Late Carboniferous to Triassic (Sengör et al., 1993; Berzin et al., 1994). It is not known whether this inversion of rotation sense affected the stress field of Central Asia.

### 5.4. Late Palaeozoic–Early Mesozoic extension

The formation of Cordilleran-type core complexes is generally believed to reflect ductile asymmetric

extension of the crust (Crittenden et al., 1980; Sturcio et al., 1983; Fournier et al., 1991). This extension does not necessarily imply the existence of a new phase of oceanic opening. It may be explained in a similar manner as for the North American Cordillera, by a combination of mechanisms which generated extensional stresses during the tectonic evolution of an active continental margin. Coney (1987) suggested as possible causes of extension: gravitational instability of overthickened crust in front of the subduction zone, stress drop due to modification in plate kinematics, and collapse and/or steepening of the subducting slab. All these proposed arguments are 'passive' factors and imply forces generated by buoyancy, by the plates themselves and by plate interactions.

Formation of the metamorphic core complexes along the Mongol–Stanovoy zone occurred diachronously, starting in the Late Permian–Early Triassic to the west and ending in the Middle–Late Jurassic to the east (Sklyarov, 1993). This can be related to the progressive eastward closure of the Mongol–Okhotsk ocean, along a northwest-dipping subduction zone (Fig. 11E, 11F). This corresponds to the palaeogeographical reconstructions of Enkin et al. (1992), based on a critical review of palaeomagnetic constraints, which show that the southeast margin of the Siberian plate (including the Palaeozoic accreted terranes) was in an active margin situation, at least from the Late Permian to the Late Jurassic.

#### *5.5. Mesozoic inversion and transpressional ramp-type basin development*

In the Early–Middle Jurassic, sedimentary basins started to develop along the margin of the Siberian platform and in the Trans-Baikal area, probably related to the last phase of Middle Mesozoic extension. After tectonic inversion in the Late Jurassic–Early Cretaceous, they evolved as ramp-type basins in a transpressive context until the beginning of the Late Cretaceous. Their development is linked to the oblique continental collision resulting from progressive closure of the Mongol–Okhotsk ocean (Fig. 11F).

Several recent papers point to the importance of basin development in a compressive setting in Central Asia, mostly for the Cenozoic period (Cobbold et al., 1993; Nikishin et al., 1993; Lobkovsky et al.,

submitted). Intraplate stress induced by plate collision is believed to control the occurrence of large-scale folds in the lithosphere. These may further evolve as a succession of ramp-type basins separated by basement uplifts. The characteristic wavelength of folds in Central Asia is about 360 km and reflects folding of the whole lithosphere. An intermediate wavelength of 30–50 km reflects the folding of the mechanically strong upper lithosphere (Nikishin et al., 1993; Burov et al., 1993). The variations of the fold wavelengths are dependent on the magnitude of compressional stress and the rheology and thickness of the lithosphere.

According to these recent developments, the Pri-Baikal foredeep and the Trans-Baikal basin system can be regarded as new Mesozoic examples of ramp-type basin development in a compressive setting, and related to lithospheric buckling, at least for their final stage of development. It was shown that the Pri-Baikal foredeep is associated to a large basement uplift in the region of Bratsk, and to an elongated Jurassic foredeep, extending into the Yakutian region, further north. The total wavelength reaches an exceptionally high value of 700 km, reflecting the great strength of the lithosphere under the Siberian platform (150–200 km thick, according to Zorin et al., 1989) and its old thermo-tectonic age. By comparison, the short 50–70 km wavelength in the Trans-Baikal region can be explained by the combined effect of a weakened and thinned lithosphere (100–150 km thick, according to Zorin et al., 1989) and a higher stress level in front of the southwestern edge of the Angara–Lena plate, indented into the Sayan–Baikal belt. A similar situation may also apply for the other Mesozoic foredeeps along the southern border of the Siberian platform, but this should be checked by additional studies.

A review of Chinese palaeomagnetic poles (including China and Mongolia), with reference to the 'stable' Eurasian apparent polar wander path (including Siberia and Kazakhstan), shows that the Mongolia–China block is still significantly far-sided with respect to Eurasia in the Late Jurassic (Enkin et al., 1992). Mongolia and China are assembled with Eurasia in the Early Cretaceous, and fully accreted to Eurasia in the Late Cretaceous. According to the position of the palaeopoles, and in present coordinates, the relative movement between Siberia and

Mongolia in the Late Jurassic was approximately in a N–S direction, similar to the mean direction of maximum horizontal palaeostress axes reconstructed for the Cretaceous period. This is in good agreement with the conclusions of Richardson (1992) showing a general correlation between directions of maximum horizontal stress and plate motion. Therefore, the typical N–S direction of compression can be regarded as an indicator of movement orientation during plate convergence for the Mongol–Okhotsk oceanic closure (Fig. 11F). In this context, the geometry of the southeastern margin of the Late Jurassic Siberian plate (including the already accreted Sayan–Baikal belt), oblique to the principal direction of plate convergence, had important consequences for the deformation mechanism in the surrounding Sayan–Baikal belt.

The oblique convergence of the Mongol–China block resulted in an initial collision of Mongolia with the Sayan–Baikal belt in the Dzhida area in the Late Jurassic to Early Cretaceous. Along the external margin of the Sayan–Baikal belt, the oceanic closure progressed in a northeast direction, from Central Mongolia to the Stanovoy area, where orogeny was active during Late Cretaceous–Paleocene time.

Jurassic–Cretaceous deformation was not confined to the zone of collision, but spread over the whole Sayan–Baikal belt, whose lithosphere was thinned and weakened by the Late Palaeozoic–Early Mesozoic extension. Deformation reached the margin of the thick and strong Siberian platform, and was even intensified along its margin (Prisayan–Angara thrust). The Angara–Lena strong cratonic plate had an indenter effect on the surrounding weakened Sayan–Baikal fold belt during the Mesozoic N–S compression. The general fault system displays a curved pattern, E-trending near the southern tip of the Angara–Lena plate and ENE-trending in Trans-Baikal. The dominant fault movement and reconstructed palaeostress tensors also vary away from the Angara–Lena plate. Along the Prisayan–Angara thrust, dip-slip reverse faulting along 30–60°-dipping faults are associated to a pure compressive stress regime (e.g., Fig. 4d, sites 100, 103, 115). In Trans-Baikal, strike-slip faulting is dominant along two sets of high-angle faults: a major set of ENE-trending sinistral strike-slip faults and a secondary set of N- to NNW-trending faults, either synthetic or

antithetic (e.g., Fig. 4d, sites 110, 116, 118 and 124). The palaeostress tensors for this area are also of an intermediate type between strike-slip and compressive types.

## 6. Conclusions

The microstructural analysis and palaeostress reconstructions for the Baikal pre-rift basement allow to recognize five major stress stages, which can be related to major tectonic events. Further correlation with preliminary results from the Altai area evidences an additional palaeostress stage, not recorded in the Baikal? timing of the palaeostress stages, is not always well constrained stratigraphically, but in most cases, a broad time bracket can be given by indirect correlations with known tectonic events. These are the first palaeostress results for this part of Central Asia, so no possibilities exist for correlation with previous results.

It should be emphasized that the detailed geodynamic evolution of Central Asia is by far more complex than reported here. Based on a systematic compilation of ages of molasse basins, blueschist occurrences and magmatism, Berzin and Dobretsov (1994) evidence up to sixteen successive tectonic stages for the Late Riphean–Late Mesozoic period. In this palaeostress investigation, it was possible to differentiate only six main stress stages for this time period. Some tectonic events reported by Berzin and Dobretsov (1994) are simply not recorded and others may be grouped together in a single palaeostress stage. This illustrates the limitations, but also the advantages of the palaeostress method. A tectonic event must be expressed by brittle microstructures in the area of investigation to be recorded as a palaeostress phase. The development of microstructures in rocks depend on the stress state itself, on the rheology of the material involved, on the presence of older lines of weakness, and on the location of the observation sites relative to the zones of main deformation. Therefore, not all stress events can be recorded adequately. The advantage of this situation is that the events recorded are generally the dominant ones, in intensity of deformation and duration of activity. There is a sort of filtering of tectonic events, which gives a simplified image of the evolution of stress fields.

Palaeostress stage 1 (Late Cambrian–Early Ordovician: Fig. 11A) corresponds to a N–S compression in brittle–ductile conditions, observed only in the Central Baikal area, along the Primorsky shear zone. This first stage is related to the closure of the Early Caledonian Palaeo-Asian oceanic branch between the Khamar Daban–Barguzin microcontinent and the Siberian platform, by lateral accretion along the southeastern margin of the Angara–Lena plate and by frontal accretion in the Vitim embayment. The oceanic evolution then shifted southwards, as indicated by the Dzhida ophiolite zone. This marks the early stage of the Palaeo-Mongol–Okhotsk oceanic evolution.

Palaeostress stage 2 (Late Silurian–Early Devonian: Fig. 11B) corresponds to a NW–SE compression all along the present western coast of Lake Baikal. It caused intense thrusting and folding in the Pri-Baikal belt, probably as a result of the first collisional–accretional activity of the Palaeo-Mongol–Okhotsk ocean, along a new subduction zone at the southeastern margin of the Khamar Daban–Barguzin block.

Palaeostress stage 3a (Late Devonian–Middle Carboniferous: Fig. 11C) was recorded only in the Altai region and corresponds to a N–S compression, linked to the progressive closure of the Palaeo-Tethys between the Kazakhstan and Altai–Mongol microcontinents.

Palaeostress stage 3b (Late Carboniferous–Early Permian?: Fig. 11D) corresponds to a E–W compression along the margin of the Angara–Lena plate, which caused dominantly strike-slip movements. This event can be related to the remote effects of the closure of the Irtysh–Zaizan branch of the Palaeo-Asian ocean in the Altai and Tien-Shan regions, southeast of the Angara–Lena plate. This stage is correlatable with an E–W compression stage observed in the Altai area, but more data are necessary to confirm this.

Palaeostress stage 4 (Late Permian–Early Triassic: Fig. 11E) corresponds to NNW–SSE extension in semi-ductile conditions, that caused the development of a belt of metamorphic core complexes and dyke swarms in the Trans-Baikal region. It is related to a Cordilleran-type of extension along the active margin of the Mongol–Okhotsk ocean.

Palaeostress stage 5 (Late Jurassic?–Late Cretaceous: Fig. 11F) corresponds to a new cycle of N–S compression, that affected only the Southern Siberian platform and the Trans-Baikal area. This stage caused the inversion of the large foredeep on the margin of the Angara–Lena plate, with the development of the Prisayan–Angara thrust, and the inversion of the Trans-Baikal basins into half-ramp or full-ramp basins. This N–S compression was caused by the closure of the Mongol–Okhotsk ocean between the Siberian plate and the Mongol–China plate.

To complete the pattern of tectonic evolution, and with reference to the tectonic stages evidenced by Berzin and Dobretsov (1994), the following stages have to be added: (1) an earlier collisional stage in Late Riphean–Vendian, related to the accretion of the Khamar Daban–Barguzin microcontinent to the Siberian platform in the Vitim area; (2) a Late Ordovician–Early Silurian stage in Mongolian Altai; (3) an additional subdivision of palaeostress 3a (Late Devonian–Middle Carboniferous) in two different tectonic events occurring in the Altai region; (4) a Middle–Late Triassic stage corresponding to the Triassic volcanism in Trans-Baikal; (5) an Early–Middle Jurassic stage corresponding to the initial development of sedimentary basins in a possible extensional context; and (6) a subdivision of palaeostress stage 5 into a Late Jurassic–Early Cretaceous stage of basin development and an Early–Late Cretaceous stage of intense compression and trachybasalt volcanism.

Recent investigations of intraplate stress field characteristics indicate that regional stress fields should contain information on plate tectonic mechanisms. In particular, a strong correlation between directions of maximum horizontal stress and absolute plate motion was demonstrated for several continental-scale regions of uniform stress fields. The present reconstructions of regional palaeostress for the Baikal basement and their remarkable consistency over the whole Baikal region allow to use the horizontal principal directions of compression as additional constraints for palaeogeodynamic reconstructions. Existing models for Palaeozoic and Mesozoic geodynamic evolution in Central Asia were adapted by assuming a possible correlation between regional horizontal palaeostress axes and plate motion. This

correlation was verified for the Mesozoic closure of the Mongol–Okhotsk ocean, by results of the independent palaeomagnetic work of Enkin et al. (1992).

Our work indicates that multiphase compressive tectonics was clearly recorded by microstructures along the southern margin of the Siberian platform. It is also clear that the pattern of palaeostress phases reflects only a part of the total tectonic history, and that all tectonic phases evidenced by the detailed geology are not differentiated here. The real situation should be much more complicated. These first results may serve as a base for further investigation in this field.

The marginal suture was very sensitive to compressive stress fields, recording most of major collisional events in Central Asia, even relatively remote ones. The succession of compressive palaeostress stages reflects the accretional–collisional history of Precambrian–Palaeozoic terranes around the Siberian platform into successive rims in Early Caledonian, Late Caledonian, Hercynian and Mesozoic times. The Trans-Baikal region only recorded the last compressive event in the Mesozoic. This is probably due to the formation of metamorphic core complexes and the widespread intrusion of Ordovician–Silurian and Devonian granites, which may have caused almost complete disappearance of earlier deformations.

The long tectonic history of the Baikal rift basement in the Palaeozoic and Mesozoic results in the constitution of a highly heterogeneous structural basement, precursor to the Cenozoic rifting (Zamaraev et al., 1979). The main Sayan and Primorsky shear zones which were established in the Late Cambrian–Early Ordovician (Stage 1) are still active today. The Primorsky shear zone strictly controlled the location of a major border fault in the Central Baikal basin and contributed to the evolution of the Academician ridge that separates the Central and North Baikal basins. The Late Silurian–Early Devonian development of reverse and thrust faults along the Pri-Baikal belt also defined suitably oriented discontinuities that were reactivated during the Cenozoic rifting. The Mesozoic activity had a strong precursor effect in the Trans-Baikal region. The Late Permian–Early Triassic crustal thinning and the subsequent tectonic inversion result in a series of ramp-type basins which were easily reactivated during the Cenozoic rifting.

## Acknowledgements

This work has been realized in the framework of the project ‘CASIMIR—Comparative Analysis of Sedimentary Infill Mechanisms in Rifts’, a joint project between the Baikal International Centre for Ecological Research (BICER) at Irkutsk (Russia) and the Royal Museum for Central Africa at Tervuren (Belgium). We thank the National Scientific Institutions of Belgium and the Siberian branch of the Russian Academy of Sciences for financial support. We are specially grateful to Academician N.A. Logatchev and J. Klerkx for promoting this research. K. Levi, A. Miroshnichenko, E. Sklyarov, N. Berzin, K. Theunissen and J.-L. Lenoir are also thanked for logistical support and/or joint field work and helpful discussions. Critical review by N. Dobretsov, F. Neubauer and an anonymous reviewer is appreciated, as well as comments by T. Perepelova on the English style.

## References

- Aftalion, M., Bibikova, E.V., Bowes, E.R., Hopgood, A.M. and Perchuk, L.L., 1991. Timing of Early Proterozoic collisional and extensional events in the granulite–gneiss–charnockite–granite complex, Lake Baikal, USSR: a U–Pb, Rb–Sr and Sm–Nd isotopic study. *J. Geol.*, 99(6): 851–861.
- Alexandrov, V.K., 1989. Thrust and nappe structures of the Pri–Baikal area. Nauka, Novosibirsk, 103 pp. (in Russian).
- Allen, M.B., Windley, B.F. and Zang Chi, 1992. Paleozoic collisional tectonics and magmatism of the Chinese Tien Shan, central Asia. *Tectonophysics*, 220: 89–115.
- Angelier, J., 1989. From orientation to magnitudes in paleostress determinations using fault slip data. *J. Struct. Geol.*, 11: 37–50.
- Angelier, J., 1991a. Inversion directe et recherche 4-D: comparaison physique et mathématique de deux méthodes de détermination des tenseurs des paléocontraintes en tectonique de failles. *C.R. Acad. Sci., Paris*, 312(II): 1213–1218.
- Angelier, J., 1991b. Deux éléments nouveaux dans l’inversion des données de tectonique cassante: les non-failles et les structures de pression/tension. *Soc. Géol. Fr., Spec. Meet., Analysis and modelling of faulting*, Paris, 9–10 déc. 1991, p. 8 (abstr.).
- Angelier, J. and Mechler, P., 1977. Sur une méthode graphique de recherche des contraintes principales également utilisable en tectonique et en seismologie: la méthode des dièdres droits. *Bull. Soc. Géol. Fr.*, 7(19): 1309–1318.
- Belichenko, V.G., Sklyarov, E.V., Dobretsov, N.L. and Tomurtogoo, O., 1994. Geodynamic map of the Paleo-Asian ocean (eastern part). *Russian Geol. Geophys.*, 35(7–8): 29–40 (Russian version).

- Berzin, N.A. and Dobretsov, N.L., 1994. Geodynamic evolution of Southern Siberia in Late Precambrian–Early Paleozoic time. In: R.G. Coleman (Editor), *Reconstruction of the Paleo-Asian Ocean*. VSP Int. Sci Publishers, Netherlands, pp. 45–62.
- Berzin, N.A., Coleman, R.G., Dobretsov, N.L., Zonenshain, L.O., Xiao, X.C. and Chang, E., 1994. Geodynamic map of the western part of the Paleo-Asian Ocean. *Russian Geol. Geophys.*, 35(7–8): 8–28 (Russian version).
- Bibikova, E.V., Karpenko, S.F., Sumin, L.V., Bogdanovskiy, O.G., Kimozova, T.I., Lalikov, A.V., Macarov, V.A., Arakelanz, M.M., Korikovskiy, S.P., Fedorovsky, V.S., Petrova, Z.I. and Levitskiy, V.I., 1990. U–Pb, Sm–Nd and K–Ar ages of metamorphic and magmatic rocks of Pri–Olkhonye (Western Pribaikaliye). In: *Geology and Geochronology of the Precambrian Siberian platform and Surrounding Fold Belts*. Nauka, Leningrad, pp. 170–183 (in Russian).
- Bothworth, W., Strecker, M.R. and Blisniuk, P.M., 1992. Integration of East African paleostress and present-day stress data: implications for continental stress field dynamics. *J. Geophys. Res.*, 97(B8): 11,851–11,865.
- Bott, M.H.P., 1959. The mechanisms of oblique slip faulting. *Geol. Mag.*, 96: 109–117.
- Bukharov, A.A., 1973. Geological Structure of the North Baikal Marginal Volcanic Belt. Nauka, Novosibirsk, 139 pp. (in Russian).
- Bukharov, A.A., Khalilov, V.A., Strakhova, T.M. and Chernikov, V.V., 1992. Geology of the Baikal–Patom upland revealed from new U–Pb dating. *Sov. Geol.*, 12: 29–39 (in Russian).
- Bukharov, A.A., Dobretsov, N.L., Zonenshain, L.P., Kuzmin, M.I. and Fialkov, A., 1993. Geological structure of middle part of Lake Baikal according to data of deep-water studies with the manned submersible ‘PISCES’. *Russian Geol. Geophys.*, 34(9): 19–30 (Russian version).
- Burov, E.B., Lobkovsky, L.I., Cloetingh, S. and Nikishin, A.M., 1993. Continental lithosphere folding in Central Asia (Part II): constraints from gravity and topography. *Tectonophysics*, 226: 73–87.
- Cloetingh, S. and Wortel, M., 1986. State of stress in the Indo–Australian plate. *Tectonophysics*, 132: 49–67.
- Cobbold, P.R., Davy, P., Gapais, D., Rossello, E.A., Sadybakasov, E., Thomas, J.C., Tondji Biyo, J.J. and Urreiztieta, M., 1993. Sedimentary basins and crustal thickening. *Sediment. Geol.*, 86: 77–89.
- Coney, P.J., 1987. The regional tectonic setting and possible causes of Cenozoic extension in the North American Cordillera. In: M.P. Coward, J.F. Dewey and P.L. Hancock (Editors), *Continental Extension Tectonics*. Geol. Soc. London, Spec. Publ., 28: 177–186.
- Crittenden, M.D., Coney, P.J. and Davis, G.H., 1980. Cordilleran metamorphic core complexes. *Geol. Soc. Am. Mem.*, 153.
- Delvaux, D., 1993. The TENSOR program for reconstruction: examples from the East African and the Baikal rift zones. *Terra Abstracts. Abstract Supplement*, 1, to *Terra Nova*, 5: 216.
- Delvaux, D., Levi, K., Kajara, R. and Sarota, J., 1992. Cenozoic paleostress and kinematic evolution of the Rukwa–North Malawi rift valley (East African rift system). *Bull. Cent. Rech. Explor. Prod. Elf Aquitaine*, 16: 383–406.
- Delvaux, D., Mazukabzov, A.M., Melnikov, A.I. and Alexandrov, V.K., 1993. Early Paleozoic compressive stress field and imbricated thrust structures along the northwestern coast of Lake Baikal (Khibelen cape). *Mus. R. Afr. centr., Tervuren (Belg.)*, Dépt. Géol. Min., Rapp. Ann., 1991–1992: 123–136.
- Delvaux, D., Moeys, R., Stapel, G., Petit, C., Levi, K., Miroshnichenko, A., Ruzhitch, V. and Sankov, V., submitted. Paleostress reconstructions and geodynamics of the Baikal region, Central Asia, Part II. Cenozoic tectonic stress and fault kinematics. *Tectonophysics*.
- Déverchère, J., Houdry, F., Solonenko, N.V., Solonenko, A.V. and San’kov, V.A., 1993. Seismicity, active faults and stress fields of the North Muya region, Baikal rift: New insights on the rheology of extended continental lithosphere. *J. Geophys. Res.*, 98(B11): 19,895–19,912.
- Dobretsov, N.L., Konnikov, E.G. and Dobretsov, N.N., 1992. Precambrian ophiolite belts of southern Siberia, Russia and their metallogeny. *Precambrian Res.*, 58: 427–446.
- Dobrzhinetskaya, L.F., Molchanova, T.V., Sonyushkin, N.E., Likhachev, A.B. and Fedorovskiy, V.S., 1992. Nappe and strike-slip plastic deformation of the metamorphic complex in Pri–Olkhonye (Western Pri–Baikalye). *Geotectonics*, 2: 58–81.
- Dupin, J.-M., Sassi, W. and Angelier, J., 1993. Homogeneous stress hypothesis and actual fault slip: a distinct element analysis. *J. Struct. Geol.*, 15: 1033–1043.
- Enkin, R.J., Yang, Z., Chen, Y. and Courtillot, V., 1992. Paleomagnetic constraints on the geodynamic history of the major blocks of China from the Permian to the Present. *J. Geophys. Res.*, 97(B10): 13953–13989.
- Ermikov, V.D., 1994. Mesozoic precursors of rift structures of Central Asia. *Bull. Centr. Rech. Explor. Prod. Elf Aquitaine*, 18(1): 123–134.
- Eskin, A.S., Kiselev, A.I. and Matison, O.R., 1988. Basic dykes in the Sharyzhalgay complex of the Early Precambrian in Pri-Baikalie. In: *Metamorphic Complex of East Siberia*. Nauka Novosibirsk, pp. 123–130 (in Russian).
- Forsyth, D.W. and Uyeda, S., 1975. On the relative importance of the driving forces of plate motion. *Geophys. J.R. Astron. Soc.* 43: 163–200.
- Fournier, M., Jolivet, L. and Goffé, B., 1991. Alpine corsica metamorphic core complex. *Tectonics*, 10: 1173–1186.
- Gibsher, A.S., Izokh, A.E. and Khain, E.V., 1993. Geodynamic evolution of northern segment of the Paleo-Asian ocean in Late Riphean–Early Paleozoic. In: N.L. Dobretsov and N.A. Berzin (Editors), *Proceedings of the 4th International Symposium of IGCP Project 283: Geodynamic Evolution of the Paleo-Asian Ocean*, Novosibirsk, 15–24 June, pp. 67–69.
- Guiraud, M., Laborde, O. and Philip, H., 1989. Characterization of various types of deformation and their corresponding deviatoric stress tensor using microfault analysis. *Tectonophysics* 170: 289–316.

- Illies, J.H., 1972. Two stages Rhinegraben rifting. In: I.B. Ramberg and E.R. Newmann (Editors), *Tectonics and Geophysics of Continental Rifts*. Kluwer, Dordrecht, pp. 62–72.
- Ilyin, V.A., 1990. Proterozoic supercontinent, its latest Precambrian rifting, breakup, dispersal into smaller continents, and subsidence of their margins: evidence from Asia. *Geology*, 18: 1231–1234.
- Jaeger, J.C., 1969. *Elasticity, Fracture and Flow*. Chapman and Hall, London (3rd ed.).
- Joffe, S. and Garfunkel, Z., 1987. Plate kinematic of the circum Red Sea — a reevaluation. *Tectonophysics*, 141: 5–22.
- Kashik, S.A. and Mazilov, V.N., 1994. Main stages and paleogeography of Cenozoic sedimentation in the Baikal rift system, Central Asia. *Bull. Centr. Rech. Explor. Prod. Elf Aquitaine*, 18(2): 453–462.
- Khain, V.E., 1990. Origin of the Central Asian Mountain belt: collision or mantle diapir. *J. Geodyn.*, 11: 389–394.
- Konnikov, E.G., 1991. On the problem of ophiolites of the Baikal–Muya belt. *Sov. Geol. Geophys.*, 32(3): 104–113.
- Konnikov, E.G., Gibsher, A.S., Izokh, A.E., Sklyarov, E.V. and Khain, E.V., 1993. Paleogeodynamics of Late Precambrian for Baikal–Muya and Sayan–Tuva–Mongolia segments of the Central Asian fold belt. In: N.L. Dobretsov and N.A. Berzin (Editors), *Proceedings of the 4th International Symposium of IGCP Project 283: Geodynamic Evolution of the Paleo-Asian Ocean*, Novosibirsk, 15–24 June, pp. 88–90.
- Kuznetsov, V.G. and Khrenov, P.M., 1982. *Geological Map of Irkutsk Territory*. 1:500,000, Ministry of Geology of USSR.
- Lobkovsky, L.I., Cloetingh, S., Volozh, Yu.A., Lankreijer, A.C., Belyakov, S.L., Groshwev, V.G., Fokin, P.A., Milanovsky, E.E., Pevzner, L.A., Gorbachev, V.I. and Korneev, M.A., submitted. Extensional basins of the F.S.U. — Structure, basin formation mechanisms and subsidence history. *Tectonophysics*, in press.
- Logatchev, N.A., 1993. History and geodynamics of the Baikal rift (east Siberia): a review. *Bull. Centr. Rech. Explor. Prod. Elf Aquitaine*, 17(2): 353–370.
- Logatchev, N.A. and Florensov, N.A., 1978. The Baikal system of rift valleys. *Tectonophysics*, 45: 1–13.
- Logatchev, N.A. and Zorin, Yu.A., 1987. Evidence and cause of the two-stage development of the Baikal rift. *Tectonophysics*, 143: 225–234.
- Logatchev, N.A. and Zorin, Yu.A., 1992. Baikal rift zone: structure and geodynamics. *Tectonophysics*, 208: 273–286.
- Manuilova, M.M. and Koltsova, T.W., 1969. Isotopic age determinations by K–Ar method. In: AZOPRO (Editor), *Geology of Pri-Baikalia*. Proceedings of the XII Session of the International Association to Study Deep Zones of the Earth Crust, Irkutsk, pp. 168–173.
- Melnikov, A.I., 1991. The Sharyzhalgay structural zone of the southern Siberian platform (Pri-Baikalye). In: O.M. Rosen (Editor), *Granulite Complexes of the Lower Continental Crust* (regional reviews). Nauka, Moscow, pp. 71–92 (in Russian).
- Melnikov, A.I., Mazukabzov, A.M., Sklyarov, E.V. and Vasiliev, E.P., 1994. Baikal rift basement: structure and tectonic evolution. *Bull. Centr. Rech. Explor. Prod. Elf Aquitaine*, 18(1): 99–122.
- Molnar, P. and Tapponnier, P., 1975. Cenozoic tectonics of Asia: effects of a continental collision. *Science*, 189(4201): 419–426.
- Mossakovsky, A.A. and Dergunov, A.B., 1985. The Caledonides of Kazakhstan, Siberia, and Mongolia: a review of structure, development history, and palaeotectonic environments. In: D.G. Gee and B.A. Sturt (Editors), *The Caledonide Orogen of Scandinavia and Related Areas*. Wiley, New York, NY, pp. 1201–1215.
- Neymark, L.A., Larin, A.M., Yakovleva, S.Z., Sryvtsev, N.A. and Buldygerov, V.V., 1991. New age data on rocks of the Akitkan Group, Baikal–Patom fold system, as revealed by U–Pb dating of zircons. *Dokl. Akad. Nauk USSR, Earth Sci.*, 321(8): 197–201.
- Neymark, L.A., Rytsk, E.Y. and Rizvanova, N.G., 1993a. Hercynian age and Precambrian crustal protolith of Barguzin granitoid of Angara–Vitim batholith: U–Pb and Sm–Nd isotopic evidence. *Dokl. RAN, Earth Sci.*, 331(6): 726–729.
- Neymark, L.A., Rytsk, E.Y., Rizvanova, N.G., Gorokhovitskiy, B.M., 1993b. On polichronicity of Angara–Vitim batholith from U–Pb method data. *Dokl. RAN, Earth Sci.*, 331(5): 634–638.
- Nikishin, A.M., Cloetingh, S., Lobkovsky, L.I., Burov, E.B. and Lankreijer, A.C., 1993. Continental lithosphere folding in Central Asia (Part I): constraints from geological observations. *Tectonophysics*, 226: 59–72.
- Ott d'Estevou, P., Jarrige, J.J., Montenat, C. and Richert, J.P., 1989. Succession des paléochamps de contrainte et évolution du rift du Golf de Suez et de la Mer Rouge nord-occidentale. *Bull. Centr. Rech. Explor. Prod. Elf Aquitaine*, 13: 297–318.
- Pollard, D.D., Saltzer, S.D. and Rubin, A., 1993. Stress inversion methods: are they based on faulty assumptions? *J. Struct. Geol.*, 15(8): 1045–1054.
- Richardson, R.M., 1992. Ridge forces, absolute plate motions and the intraplate stress field. *J. Geophys. Res.*, 97(B8): 11,739–11,748.
- Ring, U., Betzler, C. and Delvaux, D., 1992. Normal vs. strike-slip faulting during rift development in East Africa: the Malawi rift. *Geology*, 20: 115–118.
- Rundqvist, D.V. and Mitrofanov, F.P., 1993. *Precambrian Geology of the USSR*. Developments in Precambrian Geology 9, Elsevier, Amsterdam, 528 pp.
- Sengör, A.M.C., Natal'in, B.A. and Burtam, V.S., 1993. Evolution of the Altaid tectonic collage and Paleozoic crustal growth in Eurasia. *Nature*, 364: 299–307.
- Shobogorov, P.T., 1977. *Geological map of Buriatia*. 1:500,000, Ministry of Geology of USSR.
- Sklyarov, E.V., 1993. Metamorphic core complexes in folded systems of the Southern Siberia (Russia). In: N.L. Dobretsov and N.A. Berzin (Editors), *Proceedings of the 4th International Symposium of IGCP Project 283: Geodynamic Evolution of the Paleo-Asian Ocean*, Novosibirsk, 15–24 June, pp. 230–231.
- Sklyarov, E.V., Mazukabzov, A.M., Donskaya, T.V., Doronina, N.A. and Shafeev, A.A., 1994. Zagan metamorphic core complex. *Dokl. RAN*, in press.
- Soloviev, V.A., 1968. *Main Features of Mesozoic Tectonics of Baikal and Trans-Baikal Areas*. Nauka, Moscow, 127 pp. (in Russian).

- Strecker, M.R., Blisniuk, P.M. and Eisbacher, G.H., 1990. Rotation of extension direction in the central Kenya rift. *Geology*, 18: 299–302.
- Sturchio, N.C., Sultan, M. and Batiza, R., 1983. Geology and origin of Meatiq Dome, Egypt: a Precambrian metamorphic core complex? *Geology*, 11: 72–76.
- Surkov, V.S., Grishin, M.P., Larichev, A.I., Lotyshev, V.I., Melnikov, N.V., Kontorovich, A.Eh., Trofimuk, A.A. and Zolotov, A.N., 1991. The Riphean sedimentary basins of Eastern Siberia Province and their petroleum potential. *Precambrian Res.*, 54: 37–44.
- Theunissen, K., Melnikov, A., Sklyarov, E., Mazukabzov, E. and Mruma, A., 1993. The Primorskiy dislocation zone in the basement of the Cenozoic Baikal rift (Russia). *Mus. R. Afr. Centr., Tervuren (Belg.), Dépt. Géol. Min., Rapp. Ann.*, 1991–1992: 123–136.
- Twiss, R.J. and Moores, E.M., 1992. *Structural Geology*. Freeman, New York, NY, 532 pp.
- Vernikovskiy, V.A., Vernikovskaya, A.E., Nozhkin, A.D. and Ponomarchuk, V.A., 1993. Geochemistry and age of the Isakian belt ophiolites (Yenisei ridge). In: N.L. Dobretsov and N.A. Berzin (Editors), *Proceedings of the 4th International Symposium of IGCP Project 283: Geodynamic Evolution of the Paleo-Asian Ocean*, Novosibirsk, 15–24 June, pp. 138–140.
- Zamaraev, S.M., Vasiliev, E.P., Ryazanov, Mazukabzov, A.M. and Ruzhitch, V.V., 1979. Relationships between ancient and Cenozoic structures of the Baikal rift zone. Nauka, Novosibirsk, 125 pp. (in Russian).
- Ziegler, P., 1992. European Cenozoic rift system. *Tectonophysics*, 208: 91–111.
- Zoback, M.L., 1992. First- and second-order patterns of stress in the lithosphere: the World Stress Map Project. *J. Geophys. Res.*, 97: 11,703–11,728.
- Zoback, M.L. et al., 1989. Global patterns of tectonic stress. *Nature*, 341: 291–298.
- Zonenshain, L.P. and Savostin, L.A., 1981. Geodynamics of the Baikal rift zone and plate tectonics of Asia. *Tectonophysics*, 76: 1–45.
- Zonenshain, L.P., Kuzmin, M.I. and Natapov, L.Sh., 1990. *Geology of the USSR: Plate Tectonic-Synthesis*. Geodyn. Ser. 21, AGU, Washington D.C., 242 pp.
- Zorin, Yu.A., Kozhevnikov, V.M., Novoselova, M.R. and Turutanov, E.K., 1989. Thickness of the lithosphere beneath the Baikal rift zone and adjacent regions. *Tectonophysics*, 168: 327–337.
- Zorin, Yu.A., Belichenko, V.G., Turutanov, E.Kh., Kozhevnikov, V.M., Ruzhentsev, S.V., Dergunov, A.B., Filippova, I.B., Tomurtogoo, O., Arvisbaatar, N., Bayasgalan, Ts., Biambaa, Ch. and Khosbayar, P., 1993. The South Siberia–Central Mongolia transect. *Tectonophysics*, 225: 361–378.